ASIAN JOURNAL OF CIVIL ENGINEERING (BHRC) VOL. 18, NO. 1(2017)
PAGES 63-97

EARTHQUAKE PERFORMANCE OF HYBRID CONTROLS FOR COUPLED BUILDINGS WITH MR DAMPERS AND SLIDING BASE ISOLATION

S.M. Dumne[1*], M.K. Shrimali[2] and S.D. Bharti[2]
[1]Applied Mechanics Department, Government Polytechnic, Aurangabad, Maharashtra, 431 005, India
[2]Center of Disaster Mitigation and Management, Malaviya National Institute of Technology Jaipur, Rajasthan 302017, India

Received: 12 March 2016; **Accepted:** 16 July 2016

ABSTRACT

This study proposed two hybrid controls for response mitigation of adjacent buildings connected by dampers referred as coupled building of which base of taller building being isolated. These controls developed using Magnetorheological dampers in combination with Friction Pendulum System and Resilient Friction Base Isolator respectively named as, Hybrid control 1 and Hybrid control 2. Most effective hybrid control is investigated by comparing the responses obtained by hybrid controls with the responses of same coupled building with Semi-active control. Further, influence of device parameters on performance of hybrid control has been studied through parametric study. The result shows that Hybrid controls are more effective in reducing the responses compared to Semi-active control, however Hybrid control 2 perform more effective not only in response reduction but also in pounding effect.

Keywords: Hybrid control; Semi-active control; coupled building; MR damper; sliding base isolation; pounding; device parameters.

1. INTRODUCTION

The concept of connecting two dynamically dissimilar adjacent buildings achieves dual advantages of response reduction and pounding avoidance. Moreover, space available between two adjacent buildings is utilized effectively for installation of device, controller etc. Mutual pounding between adjacent buildings in close proximity particularly in urban landscape becomes serious concern which can be attributed due to difference in dynamic characteristics

*E-mail address of the corresponding author: smdumne@gmail.com (S.M. Dumne)

of buildings along with lesser gap between adjacent buildings [1]; therefore efforts are being made by researchers to control pounding by installing energy controlling devices in the gap between adjacent buildings. In the past, proposed coupling devices were either passive or active type of which passive coupling is limited to a specific range of vibration modes whereas active devices needs an external energy but sometimes may be useless in case of power cut [2]. These observations have motivated the researchers to use Semi-active devices that have the advantage of combining passive and active characteristics to overcome the problems as noted. Further in succession of research [3], superiority of sliding base isolation system for its ability to control seismic response over wide range of frequency of ground motion input. For the versatility and effectiveness of Semi-active MR damper [4], seismic hazard mitigation of asymmetrically planned building model with single bay, first storey rigidly connected by MR dampers is considered for study. It is noted that MR damper-based control strategy is effective in reducing the seismic response of plan asymmetrical building.

In the past, major earthquakes such as Mexico City earthquake, 1985, Kobe earthquake, 1994, Bhuj earthquake, 2001 and recently Christchurch earthquake, 2011 are occurred. After the 1985 Mexico City earthquake, many cases of pounding between adjacent structures were reported. In a report published [5] in 1987, it has been observed that mutual impact of adjacent buildings led to significant damage in large scale during earthquake. Further, it was also revealed that adjacent buildings were having a high risk of pounding and more than 15% of the buildings which collapsed during Mexico City earthquake, were subjected to significant mutual impact. In the recent past, various approaches of seismic hazard mitigation of closely spaced adjacent buildings, by way of interconnecting through energy controlling devices, referred as coupled building control gained popularly. Thus, coupled building control is one of the techniques to connect the buildings in cluster to reduce the responses as well as pounding effect [6]. Further, this scheme may be useful, if a new building comes up adjacent to the existing isolated building and also, space available between two adjacent buildings is utilized for the installation of devices. Mean while, fluid dampers were studied [7] were found quite effective in controlling the seismic response by interconnecting two adjacent buildings using Maxwell model. Further, optimum parameters of Maxwell model [8] were determined by deriving analytical formulae and defined the fluid dampers to link two adjacent structures using the principle of average vibration energy under white noise ground excitation. The results show that fluid dampers with Maxwell model can reduce the seismic response of both structures. The study of dynamic characteristics and seismic responses of connected building models with linear viscoelastic dampers, namely as, both buildings are isolated and only shorter building is isolated [9]. The result implies that this scheme is useful in reducing the responses as well as large bearing displacement. It is also noted that seismic performance to be effective when base of one building have isolated and other fixed base. Moreover, one can use this scheme to upgrade the seismic performance of existing building adjacent to the newly constructed building. Another type of passive friction dampers is used [10] to mitigate the seismic response of connected buildings with different dynamic characteristics. The study illustrates that friction dampers are quite effective in reducing the responses and it is also observed through parametric study that it is not necessary to connect all floors of adjacent buildings by dampers but lesser dampers at appropriate locations can significantly reduce the earthquake effects. Most dynamically varied type of damper is the semi-active MR damper has

been studied [11] for their effectiveness using two adjacent RC buildings of dissimilar in characteristics are connected by in-line MR dampers under three control strategies, namely, passive-off, passive-on and Semi-active control due to four real earthquake ground motions. Based on the results, it has been observed that MR damper is an effective device to control the response of both buildings however, it was found to be more effective when shorter building was isolated, with significant response reduction taking place in taller building. Also, it was observed that significant response control is possible with passive-on strategy, which demonstrates the effectiveness of MR damper, even if control algorithm fails. Various impact simulation techniques has been presented [12] for the comparative study of pounding response of multi-degree-of-freedom (MDOF) system. The prediction of impact response of three adjacent MDOF stick system is carried out by means of spring-dashpot contact element. The result indicates that nonlinear contact spring impact simulation model gives lesser pounding forces than that of linear contact spring impact simulation model, but as far as their numbers are concerned, they are marginally same for both the types. It is also noticed that top storey of exterior rigid structure during pounding may offer more values of shear forces than the immediately lower storeys. Further, a fuzzy logic controller [13] is used to synchronize the response and minimize the top floor displacement and maximum drift to avoid the pounding of two adjacent buildings coupled by a magneto-rheological (MR) damper. It was observed that adapting a coupling strategy allows the transformation of two separated structures into one system coupled by a damping device, which results in a synchronised vibrating mode between the coupled structures. It is also noted that use of single damper at the top floor reduces response and avoid pounding. A recent, study [14] discusses seismic performance of coupled building controls connecting in-line floors of adjacent dissimilar buildings by MR dampers of which taller building is isolated by elastomeric bearing with and without lead core, subjected to unidirectional excitation due to four real earthquakes. The results established that these strategies are not only efficient to control seismic response, but also reduce the pounding phenomenon. It is also observed through parametric study that there exists an optimum location of damper connectivity and a suitable value of maximum command voltage supplied to the MR damper. Another study [15] examines the seismic performance of two Coupled Building models, in comparison with the individual building of same Coupled Building model under unidirectional excitation due to Kobe 1995 earthquake. From these two building models, one is of two adjacent buildings connected with in-line MR dampers while the other having base of taller building isolated by the Resilient-Friction Base Isolator. It is observed that second model performs more effective in controlling seismic response however, first model works effectively in avoiding impact. Further, there is significant reduction in responses of isolated building whereas marginal in fixed base building.

This study investigates the seismic performance of hybrid controls in comparison with Semi-active control, using two adjacent buildings connected by Magnetorheological (MR) dampers, of which base of taller building is being isolated by sliding base isolation systems whereas base of shorter as fixed. The controls used, namely, are Semi-active control: adjacent buildings are connected at the floor levels through in-line MR dampers, Hybrid control 1: besides inline MR dampers, taller building is isolated at the base level with Friction Pendulum System (FPS) and Hybrid control 2: besides in-line MR dampers, taller building is isolated at the base level by Resilient-Friction Base Isolator (R-FBI). The

coupled building system is subjected to unidirectional excitation, for which four real earthquake ground motions, namely, Imperial Valley, 1940 (PGA= 0.348g), Loma Prieta, 1989 (PGA= 0.57g), Kobe, 1995 (PGA= 0.837g) and Northridge, 1994 (PGA= 0.843g) are considered. Further, influence of bearing parameters such as damping, friction coefficient, period, simillarly, for damper parameters such as command voltage and location, on control performance have been investigated through parametric study. The specific objectives are, (1) investigation of most effective hybrid control not only in reducing the seismic response but also controlling pounding (2) comparing hybrid controls with the Semi-active control in terms of peak responses of interest (3) observe the variation of isolation parameters on performance of hybrid controls (4) observe the variation of damper command voltage and damper location on seismic performance of hybrid controls (5) observe the dynamic behaviour of damper and isolation system during excitation due to earthquakes.

2. STRUCTURAL MODELING OF COUPLED BUILDINGS

The coupled building consist of ten and eight storey adjacent buildings with fixed base connected by in-line MR dampers is shown in Fig. 1. Further, same couple building is modified as taller building being isolated at its base as shown in Fig. 2. As seen that only base of taller building is isolated in order to enhance the dynamic dissimilarity between two connected buildings. The floors of both buildings are at same level and number of stories in taller and shorter buildings are m and n ($m>n$) respectively. The coupled building is considered as shear type having lumped mass system with ($m+n+1$) degrees-of-freedom. The horizontal resistance of floors is assumed to be so large, that does not affect the damper performance significantly and effect of soil-structure interaction is neglected. The governing equations of motion for coupled building with controls is given as,

$$[m]\{\ddot{u}\}+[c]\{\dot{u}\}+[k]\{u\}=[P_d]\{F_d\}+[P_I]\{F_b\}-[m]\{r\}\ddot{u}_g \tag{1}$$

where, [m], [c] and [k] are the mass, damping and stiffness matrices, respectively. The displacement vector with respect to the ground is expressed as: $\{u\}= \{u_b, u_1, u_2, u_3, \ldots\ldots\ldots u_{m+n+1}\}$ in which u_b is bearing displacement and response of taller building lies in the first (m+1) positions and that of shorter building in last (n) positions; acceleration and velocity vectors are denoted by $\{\ddot{u}\}$ and $\{\dot{u}\}$, respectively. Further, $\{r\}$ is influence vector with all elements equal to unity; $\ddot{u}_g$ is ground acceleration vector; [P_d] and [P_I] are vectors for the position of damper and isolator, respectively; $\{F_d\}$ is damper force vector, and $\{F_b\}$ is bearing force vector. The mass, stiffness and damping matrices of entire coupled building are expressed as

$$[m]=\begin{bmatrix}[m_1] & [o_1]\\ [o_2] & [m_2]\end{bmatrix},\quad [k]=\begin{bmatrix}[k_1] & [o_1]\\ [o_2] & [k_2]\end{bmatrix} \text{ and } [c]=\begin{bmatrix}[c_1] & [o_1]\\ [o_2] & [c_2]\end{bmatrix}$$

where, $[o_1]_{(m+1,\ m+1)}$ and $[o_2]_{(n,\ n)}$ are the null matrices of taller and shorter building respectively. The mass matrices, $[m_1]_{(m+1,\ m+1)}$ and $[m_2]_{(n,n)}$ for the taller and shorter building respectively; stiffness matrices, $[k_1]_{(m+1,\ m+1)}$ and $[k_2]_{(n,\ n)}$ for the taller and shorter building, respectively, and damping matrices, $[c_1]_{(m+1,\ m+1)}$ and $[c_2]_{(n,\ n)}$, for the taller and shorter building, respectively. The notations used in above matrices in which first and second subscript denotes degrees-of-freedom and building number, respectively.

The governing equation of motion (1) is expressed in state-space form as

$$\{\dot{z}_1(t)\} = [A]\{z_1(t)\} + [B_d]\{d_f(t)\} + [B_b]\{b_f(t)\} + [E]\ddot{u}_g(t) \tag{2}$$

where, z_1 is the state variable, A is the system matrix composed of structural mass, stiffness and damping, Bd and Bb are distribution matrices of damper and bearing force, respectively; E is the matrix of excitation force. The matrices are explicitly expressed as

$$\dot{z}_1 = \begin{bmatrix} \dot{u} \\ \ddot{u} \end{bmatrix};\ z_1 = \begin{bmatrix} u \\ \dot{u} \end{bmatrix};\ A = \begin{bmatrix} o & I \\ -m^{-1}k & -m^{-1}c \end{bmatrix};\ B_d = \begin{bmatrix} o \\ m^{-1}P_d \end{bmatrix},\ B_b = \begin{bmatrix} o \\ m^{-1}P_1 \end{bmatrix} \text{ and } E = \begin{bmatrix} o \\ -r \end{bmatrix}$$

where, $[I]$ and $[o]$ are identity and null matrices, respectively; vector $\dot{z}_1$ (t) represents the state variable of structural system which contains relative velocity and acceleration response of structure with respect to ground.

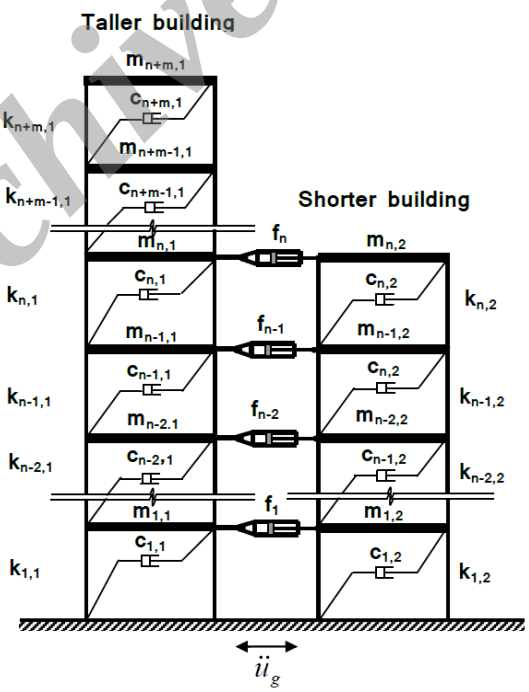

Figure 1. Coupled building model with Semi-active control

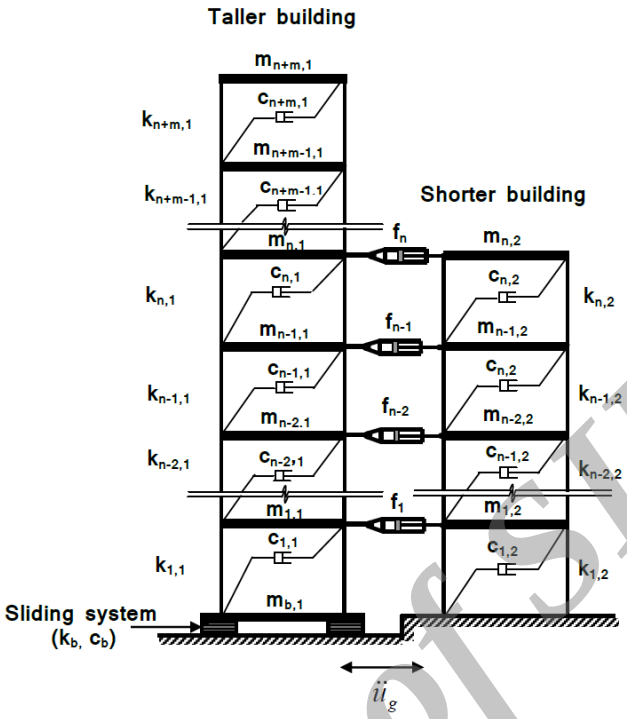

Figure 2. Coupled building model with hybrid controls

3. DYNAMIC BEHAVIOUR OF MR DAMPER

In this study, modified Bouc-Wen model [16] is used to simulate the dynamic behavior of MR damper. The cross-section [17] and its schematic diagram are shown in Fig. 3 which yield a force is given by

$$F_d = c_1\dot{x} + k_1(u_d - x_0) \tag{3}$$

where

$$\dot{x} = \left\{\frac{1}{(c_0 + c_1)}\right\}\{\alpha_0 z + c_0\dot{u}_d + k_0(u_d - x)$$

$$\dot{z} = -\gamma|\dot{u}_d - \dot{x}|(z)|z|^{(n-1)} - \beta(\dot{u}_d - \dot{x})|z|^n + A_d(\dot{u}_d - \dot{x})$$

where, u_d is the damper displacement, x is the internal pseudo-displacement of damper; z is the hysteretic displacement of damper that accounts for history dependence of response; k_1 is the accumulator stiffness; c_0 is introduced to control the viscous damping of damper at large velocities, c_1 is the viscous damping used to produce non-linear roll-off in the force-velocity

loop at low velocities**;** k_0 is introduced to control the stiffness of damper at large velocities; x_0 is the initial displacement of linear spring k_1; α_0 is the evolutionary coefficient and γ, β, n and A_d are the damper parameters that controls the shape of hysteresis loop and dot (·) represents the first derivative with respect to the time. The model parameters depends on command voltage, c_0, c_1, α_0, are expressed as

$$c_0 = c_{0a} + c_{0b}U \text{ , } c_1 = c_{1a} + c_{1b}U \text{ and } \alpha_0 = \alpha_{oa} + \alpha_{ob}U$$

where, U is the output of first order filter and given by the equation as

$$\dot{U} = -\eta(U - V) \tag{4}$$

The equation (4) is necessary to model the dynamics involved in reaching rheological equilibrium and in driving the electromagnet in damper. A small time lag exists between the command signals and damper force due to inductance in coil of electromagnet available in MR damper. This time lag is modeled by the following first-order filter equation between maximum commands voltage applied (V_{max}) and output of first-order filter *(U)* using time constant (1/η) of first order filter.

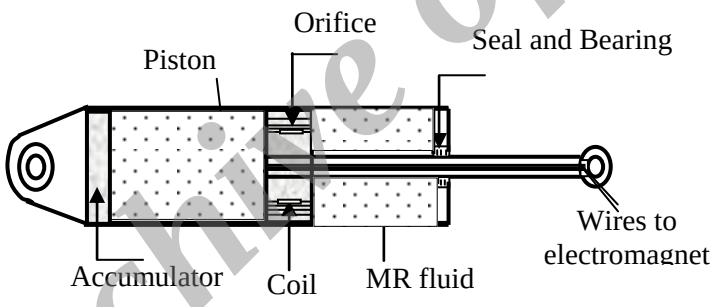

(a) Cross section of small scale MR damper

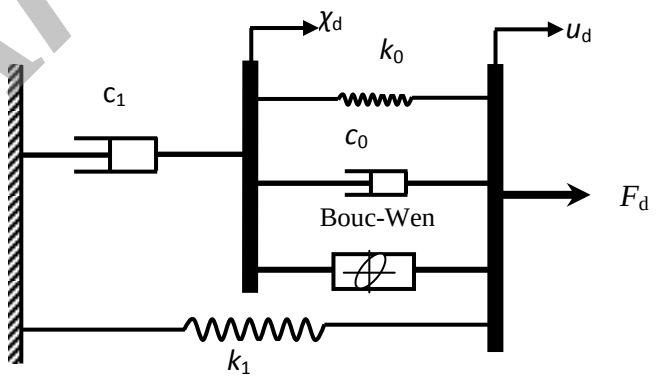

(b) Schematic representation of Modified Bouc-Wen model

Figure 3. Semi-active magnetorheological (MR) damper (Spencer et al. 1997)

Control Algorithm

The Lyapunov direct approach has been employed as a control algorithm for the stability analysis and design of controller. This theory requires the use of Lyapunov function, denoted by $L(\{z_1\})$, which must be a positive definite function of state of the system $\{z_1\}$. According to fundamental approach of Lyapunov theory, if the rate of change of Lyapunov function $L(\{z_1\})$ is negative semi-definite function, the origin is stable in the sense of Lyapunov. Thus, in determining the control law, goal is to choose a control input, which will result in making $\dot{L}$ as negative as possible. In this approach, a Lyapunov function is so chosen of the form as below

$$L(\{z_1\}) = \frac{1}{2}\left\|\{z_1\}\right\|_p^2 \tag{5}$$

The term $\left\|\{z_1\}\right\|_p$ is the P-norm of state defined by $\left\|\{z_1\}\right\|_p = \left[\{z_1^T\}[P_L]\{z_1\}\right]^{1/2}$ where, $[P_L]$ is real, symmetric, positive definite matrix and in case of a linear system, to ensure $\dot{L}$ as negative definite then $[P_L]$ is found out from the Lyapunov equation as below

$$[A^T][P_L] + [P_L][A] = -[Q_P] \tag{6}$$

For a positive definite matrix, $[Q_P]$ is considered as a unit matrix. The derivative of Lyapunov function for the solution of state-space equation is

$$\dot{L} = -\frac{1}{2}\{z_1^T\}[Q_P]\{z_1\} + \{z_1^T\}[P_L][B_d]\{F_d\}[B_b]\{F_b\} + \{z_1^T\}[P_L][E]\ddot{u}_g \tag{7}$$

In developing the control law, command voltage (V) supplied to the MR driver is restricted to either zeros or maximum, that is, $V \in [0, V_{max}]$ corresponding to a fixed set of states. Then control law which will minimize $\dot{L}$ as

$$V = V_{max} H\left(\{-z_1^T\}[P_L][B_d]\{F_d\}[B_b]\{F_b\}\right) \tag{8}$$

where, $H(\cdot)$ is Heaviside step function, when the function $H(\cdot)$ is greater than zero, command voltage supplied to the MR driver is maximum ($V = V_{\max}$) otherwise, the command voltage set to zero ($V = 0$).

4. DYNAMIC BEHAVIOUR OF FRICTION PENDULUM SYSTEM

This system is equipped with re-centering force provided by gravitational action is achieved

by means of an articulated slider moves on spherical concave chrome surface. The residual displacement after an earthquake is reduced due to self-centering action. The Fig. 4 shows cross-section and schematic diagram of Friction Pendulum System (FPS) provides isolation effect through parallel action of friction and restoring spring force by geometry. The bearing force produced by this system is given by

$$f_b = k_b u_b + f_r \tag{9}$$

where, k_b is the stiffness of bearing provided through inward gravity action, u_b is the bearing displacement, f_r is the frictional force generated at the interface of isolation system is obtained by hysteretic approach as

$$f_r = f_s \times z \tag{10}$$

where, f_s is the limiting frictional force is expressed by $f_s = \mu M_t g$ in which M_t is the total mass of building including mass of isolation floor, g is the gravitational acceleration and μ is the friction coefficient of sliding system that depends on the instantaneous velocity of base floor. The friction coefficient (μ) of sliding system with Teflon-steel bearing can be modelled [18] by using an equation is described below

$$\mu = \mu_{max} - (\Delta\mu) exp(-a|v_b|) \tag{11}$$

where, μ_{max} is the maximum friction coefficient at large velocity of sliding (after leveling off), μ_{min} is the minimum friction coefficient at small velocity of sliding, $\Delta\mu$ is the difference of maximum and minimum friction coefficient respectively at large and small velocity at the interface of system, and its value is assumed to be independent of relative velocity ($\Delta\mu=0$) at the sliding interface which leads to coulomb-friction idealization**,** a is the calibration coefficient or constant for a given bearing pressure and interface condition is taken as 20 sec/m and z is the hysteretic displacement evaluated by the Wen's model [19], satisfying the nonlinear first order differential equation as

$$q\dot{z}_b = -\beta|v_b|\,z_b\,|z_b|^{n-1} - \tau v_b\,|z_b|^n + A v_b \tag{12}$$

where, q is the yield displacement of bearing, β and τ are the strengthening coefficient of lead plug that controls the shape and size of hysteresis loop, n and A are the integer constant that controls the smoothness of transition from elastic to plastic state. The parameters β, τ, n and A are so selected so as to provide a rigid-plastic shape (typical Coulomb-friction behaviour).

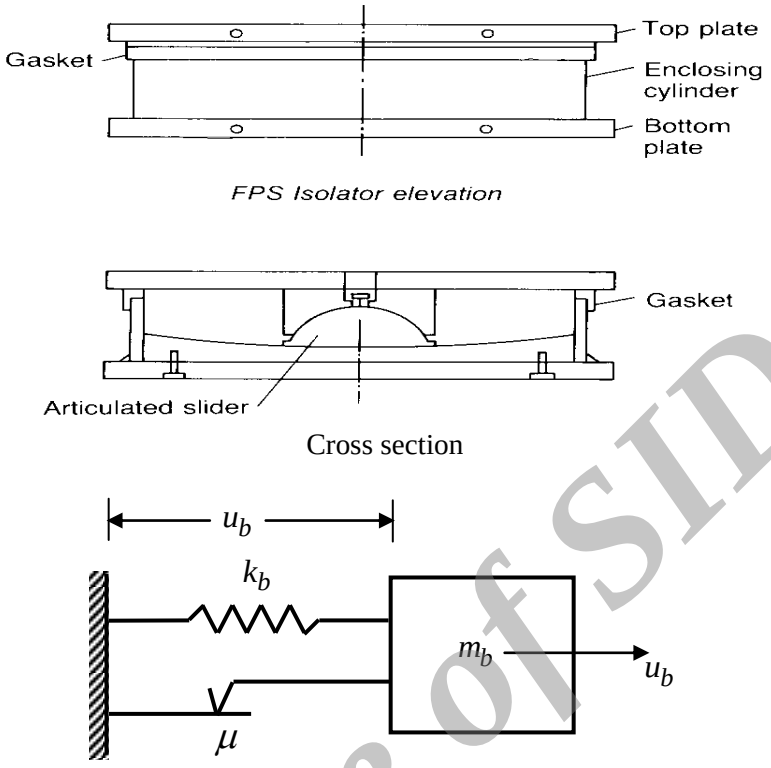

Figure 4. Friction Pendulum System

5. RESILIENT-FRICTION BASE ISOLATOR

The Resilient-Friction Base Isolator (R-FBI) is developed by the scientist Mostaghel and Khodaverdian which provides an isolation effects through parallel action of friction, damping and restoring spring as shown in Fig. 5. As soon as ground motion exceeds certain level, lateral load exceeds the friction force then base starts to slide and rubber core deforms and builds resistance. The bearing force as described [20] is given by

$$f_b = c_b v_b + k_b u_b + f_r \tag{13}$$

where, c_b and k_b are the damping and stiffness of base isolator, respectively, v_b and u_b are the velocity and displacement of bearing system respectively, f_r is the friction force produced at the interface of sliding system is obtained from the equation (Eq. 10). The stiffness (k_b) and damping ratio (ξ_b) of R-FBI are so selected to obtain the desired value of isolation period (T_b) and damping (c_b).

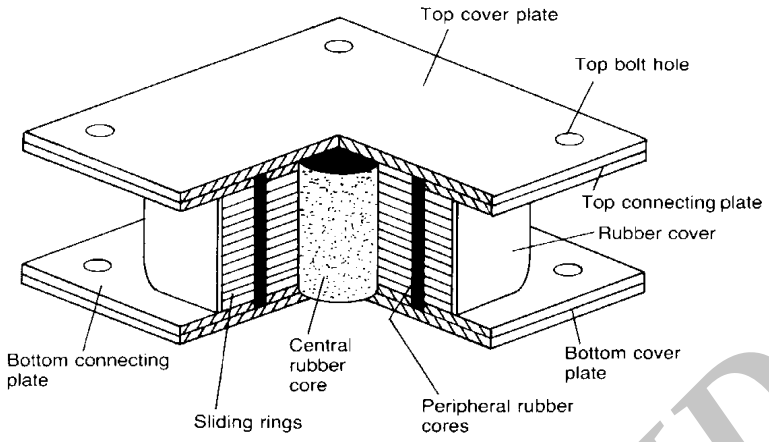

Cross-section

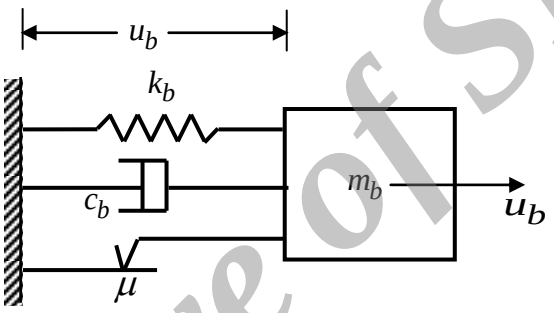

Schematic diagram

Figure 5. Resilient-friction base isolator

6. NUMERICAL STUDY

For the purpose of numerical study, two adjacent shear buildings having their structural properties such that fundamental natural period of taller and shorter buildings yielded to 0.48s and 0.39s respectively that implies their modes are well separated. The structural coupled building model used for the performance of proposed controls consists of two adjacent RC buildings having ten and eight storeys, designated as taller building and shorter building, respectively. Both the buildings have identical storey height, storey stiffness and floor mass of which each floor of shorter building are connected by in-line MR dampers and base of taller building is isolated by sliding isolation system. The floor mass and member stiffness are taken as 1600 ton and 1.2×10^7 kN/m, respectively whereas mass of isolation floor considered as 10% in excess of floor mass. The MR damper parameters are: η= 195s$^{-1,}$ c_{1a}= 8106.20 kN-s/m, c_{1b}= 7807.90 kN-s/m/V, c_{0a}= 50.30 kN-s/m, c_{0b}= 48.70 kN-s/m/V, α_{0a}= 8.70 kN/m, α_{0b}= 6.40 kN/m/V, γ= 496m^{-2}, β= 496 m^{-2}, A_d= 810.50, n= 2, k_0= 0.0054

kN/m, χ_0= 0.18 m, k_1= 0.0087 kN/m so as to yield maximum damper force using appropriate damper command voltage 6 volts. The appropriate parameters of FPS is taken as T_b= 2s and μ_{max}= 0.05; whereas for R-FBI systems, Tb= 4s, ξ_b= 0.1 and μ_{max}= 0.04. The coupled building system is subjected to unidirectional excitation, for which four real earthquake ground motions, named as EQ1, EQ2, EQ3 and EQ4 respectively for the Imperial Valley, 1940 (PGA= 0.348g), Loma Prieta, 1989 (PGA= 0.57g), Kobe, 1995 (PGA= 0.837g) and Northridge, 1994 (PGA= 0.843g) are considered. The displacement and acceleration response spectra for the four considered ground motions corresponding to 5% of critical damping are shown in Fig. 6. The peak response parameters of interest for study are considered as, top floor displacement (u_f), acceleration (a_f), bearing displacement (u_b), and base shear (B_{sy}). The base shear, bearing force, damper force and friction coefficient are normalized by the coupled building weight, weight of taller building, weight of shorter building and maximum coefficient of friction respectively.

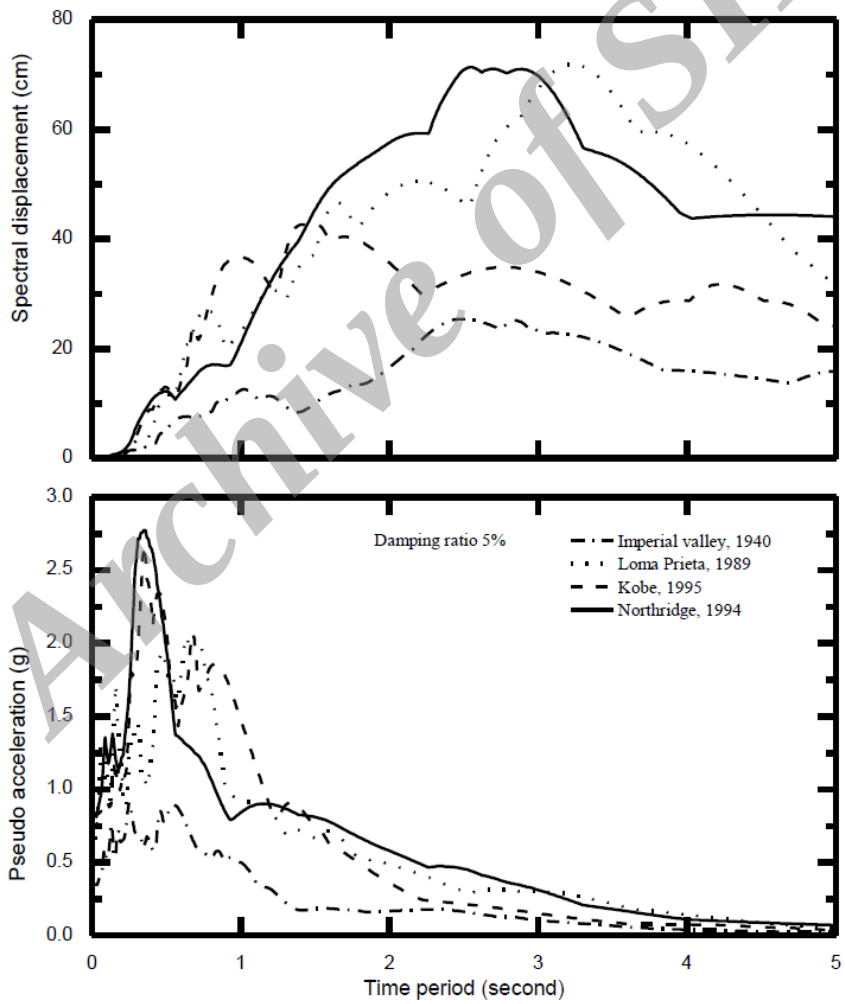

Figure 6. Response spectra of considered earthquake ground motions

The seismic performance of hybrid controls namely, Hybrid control 1 and Hybrid control 2 in terms of peak responses are compared with respect to the peak responses obtained from using Semi-active control are noted in Table 1.

Table 1: Comparative performance of hybrid controls for coupled buildings

Earthquake	Peak response	Taller building			Shorter building		
		Semi-active control	Hybrid control1	Hybrid control 2	Semi-active control	Hybrid control1	Hybrid control 2
EQ1	u_f	5.702	0.788 (86.18)	0.527 (90.75)	2.939	2.714 (07.65)	2.712 (07.72)
	a_f	1.064	0.221 (79.22)	0.187 (82.42)	0.926	0.888 (04.10)	0.889 (03.99)
	B_{sy}/W	0.700	0.120 (82.85)	0.083 (88.14)	0.566	0.532 (06.00)	0.531 (06.18)
	u_b	--	5.178	05.202 (-00.48)	--	--	--
EQ2	u_f	14.22	2.253 (84.15)	1.086 (92.36)	5.795	5.602 (03.33)	5.592 (03.50)
	a_f	2.284	0.427 (81.30)	0.257 (88.74)	1.655	1.632 (01.38)	1.627 (01.69)
	B_{sy}/W	1.771	0.302 (82.94)	0.184 (89.61)	1.082	1.074 (00.74)	1.073 (00.83)
	u_b	--	22.122	28.557 (-29.08)	--	--	--
EQ3	u_f	15.86	1.589 (89.98)	0.901 (94.31)	10.72	10.52 (01.86)	10.51 (01.86)
	a_f	2.693	0.312 (88.41)	0.268 (90.04)	2.686	2.673 (00.48)	2.671 (00.55)
	B_{sy}/W	1.898	0.211 (88.88)	0.149 (92.14)	1.944	1.924 (01.02)	1.922 (01.13)
	u_b	--	11.767	10.161 (13.64)	--	--	--
EQ4	u_f	15.63	2.393 (84.68)	1.174 (92.48)	12.95	12.60 (02.70)	12.57 (02.93)
	a_f	2.694	0.400 (85.15)	0.272 (89.90)	3.449	3.383 (01.91)	3.380 (02.00)
	B_{sy}/W	1.788	0.310 (82.66)	0.193 (89.20)	2.313	2.270 (01.86)	2.265 (02.07)
	u_b	--	22.23	18.782 (15.51)	--	--	--

Note: Value in parenthesis represents the percentage reduction in response with respect to Semi-active control in which –ve sign indicates the increase in response.

The values in parenthesis indicate the percentage reduction in response as compared to Semi-active control. It is observed that Hybrid controls manifest significant reduction in responses as compared to Semi-active control. The percentage reduction in response is in the range of 80-90% for taller building; whereas in case of shorter building, it is 1-7%. Moreover, time varying accelerogram for various cases are also drawn for, top floor displacement, acceleration and base shear responses using three considered control strategies for taller building are shown respectively through Figs. 7-9. From these figures, it is observed that significant reduction in displacement, acceleration and base shear under hybrid controls as compared to Semi-active control. Similarly, control performance for shorter building is depicted through Figs. 10-12; it is noted that these controls performs marginally better as compared to Semi-active control. Further, it is also noted that reduction in top floor responses and base shear under Hybrid control 1 and 2 are in close vicinity however, Hybrid control 2 exhibits better reduction in bearing displacement except Loma Prieta, 1989 earthquake. Further, peak displacement and acceleration at each floors of taller building are shown in Figs. 13 and 14, respectively whereas Figs. 15 and 16 shows for shorter building. From these figures, it is noted that same trend is observed as obtained in graphs of time varying response.

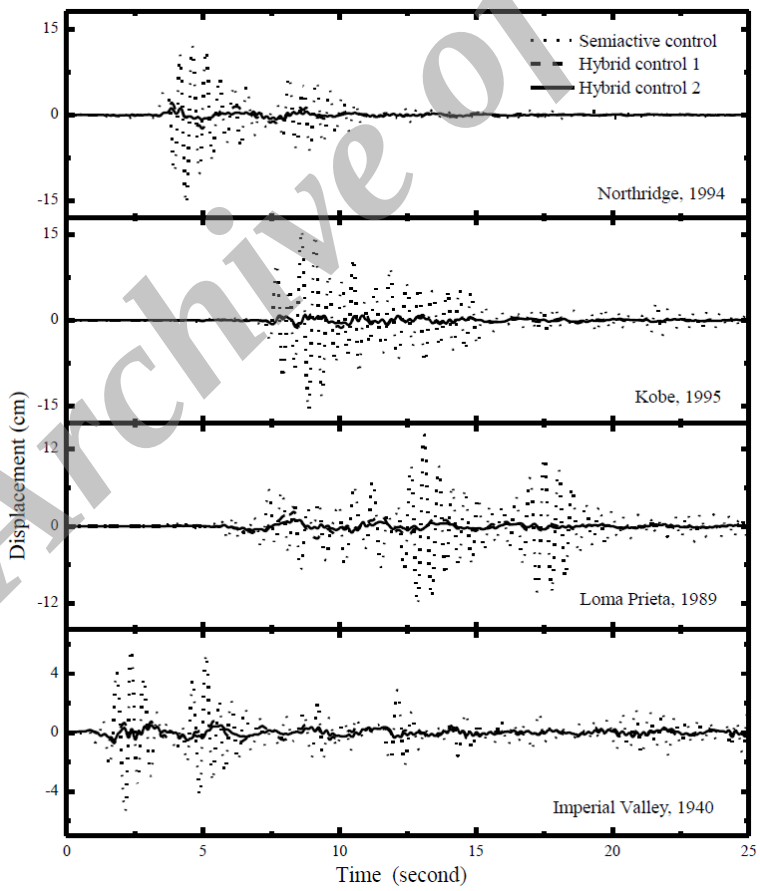

Figure 7. Time varying top floor displacement of taller building

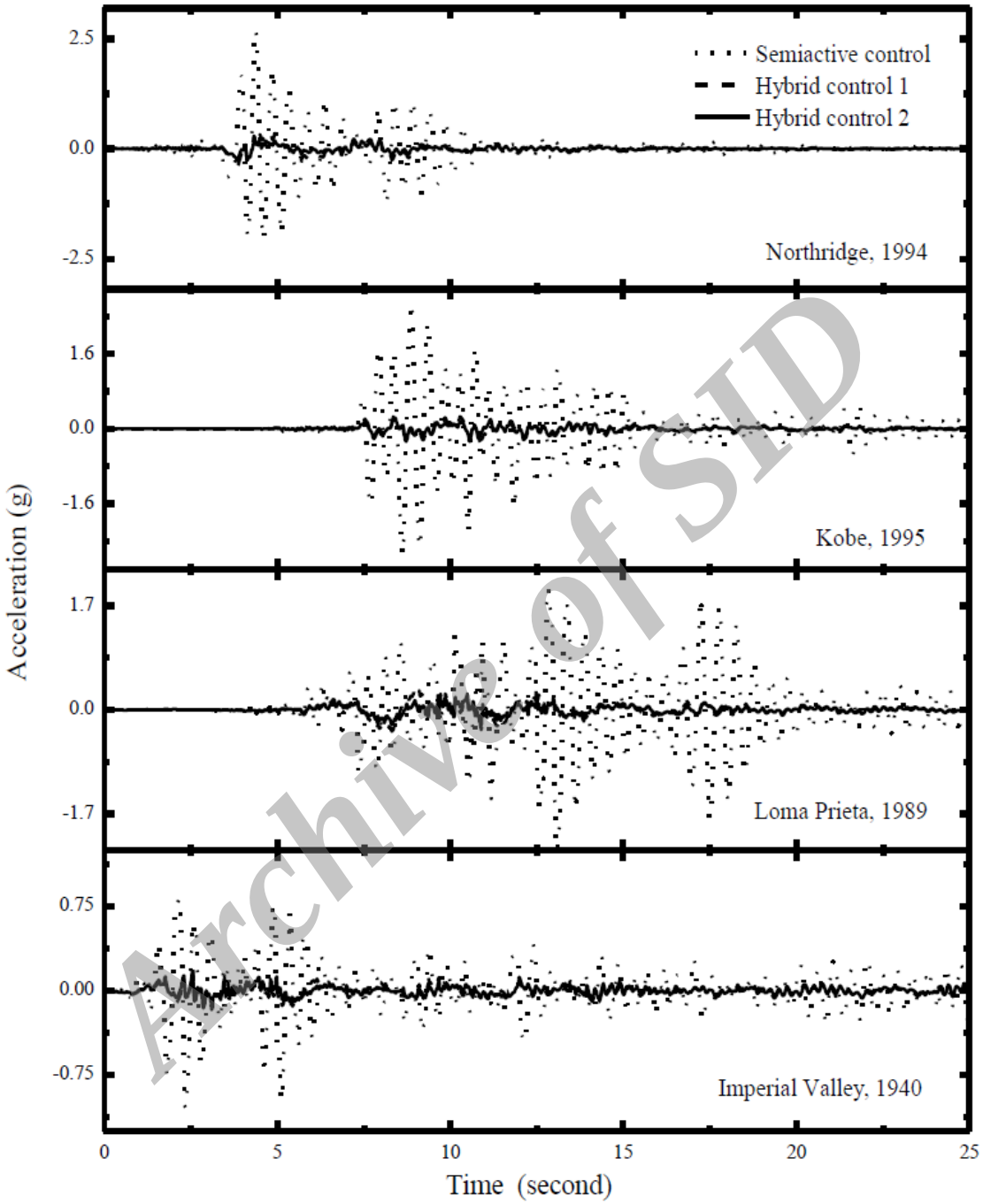

Figure 8. Time varying top floor acceleration of taller building

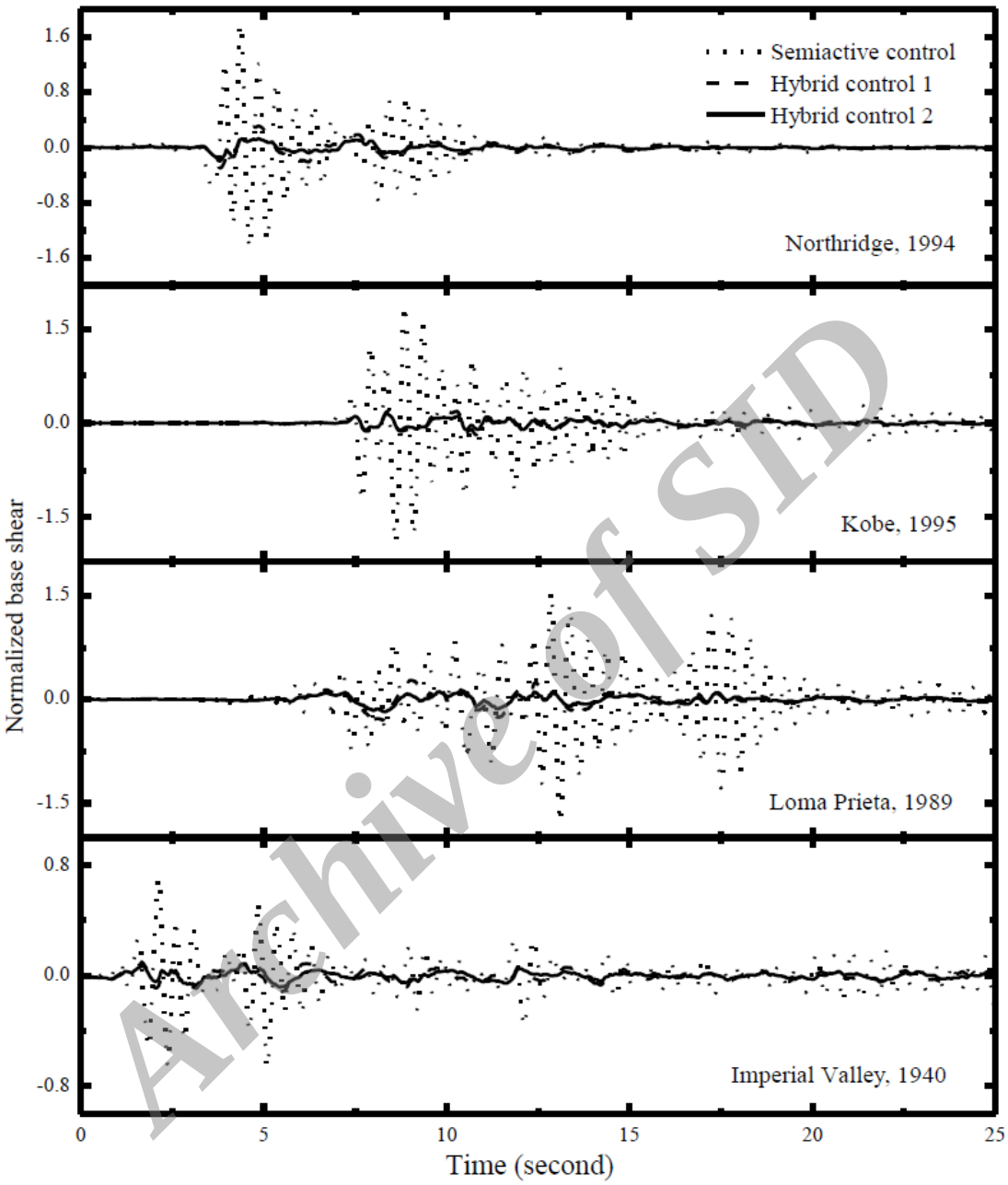

Figure 9. Time varying base shear of taller building

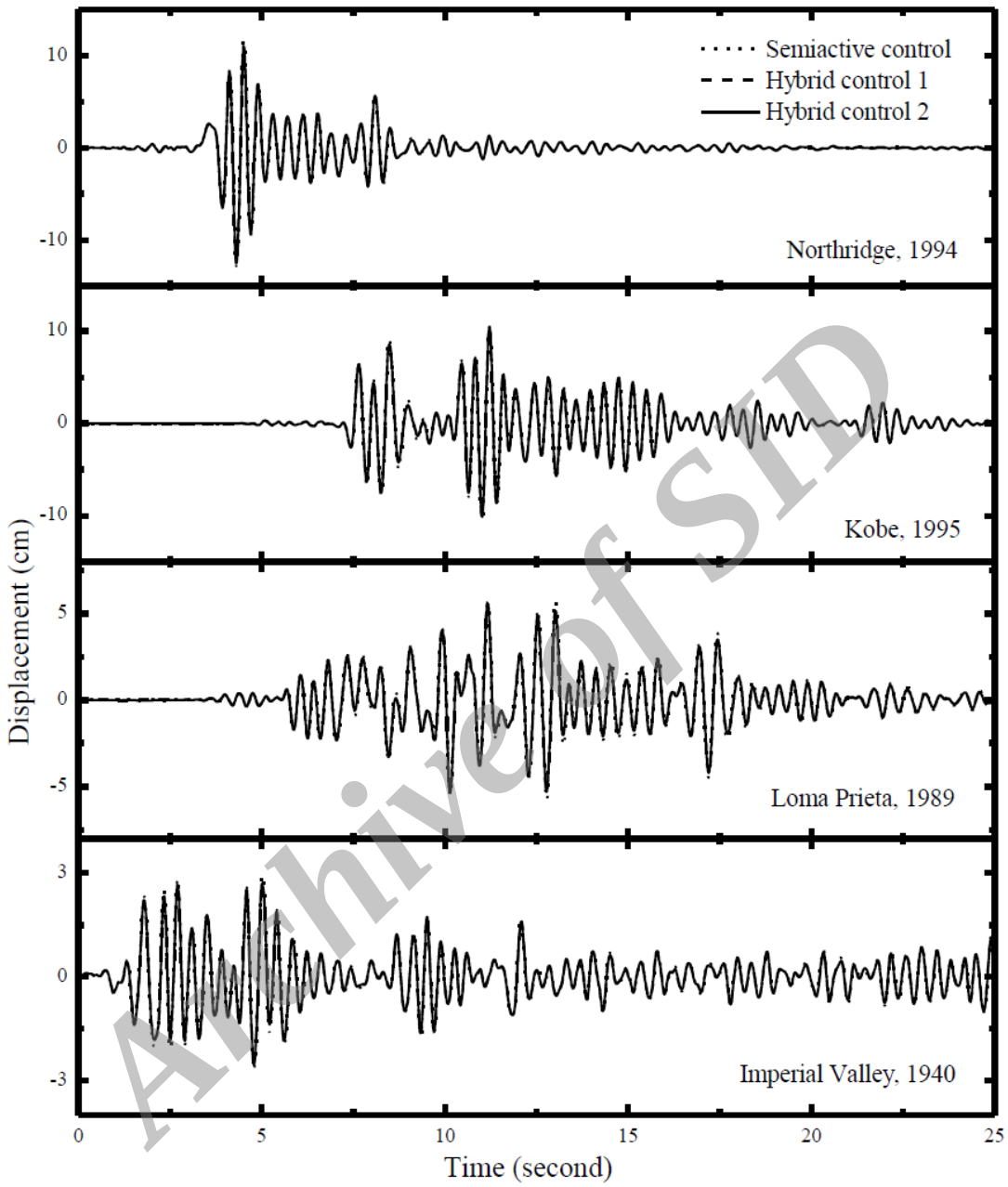

Figure 10. Time varying top floor displacement of shorter building

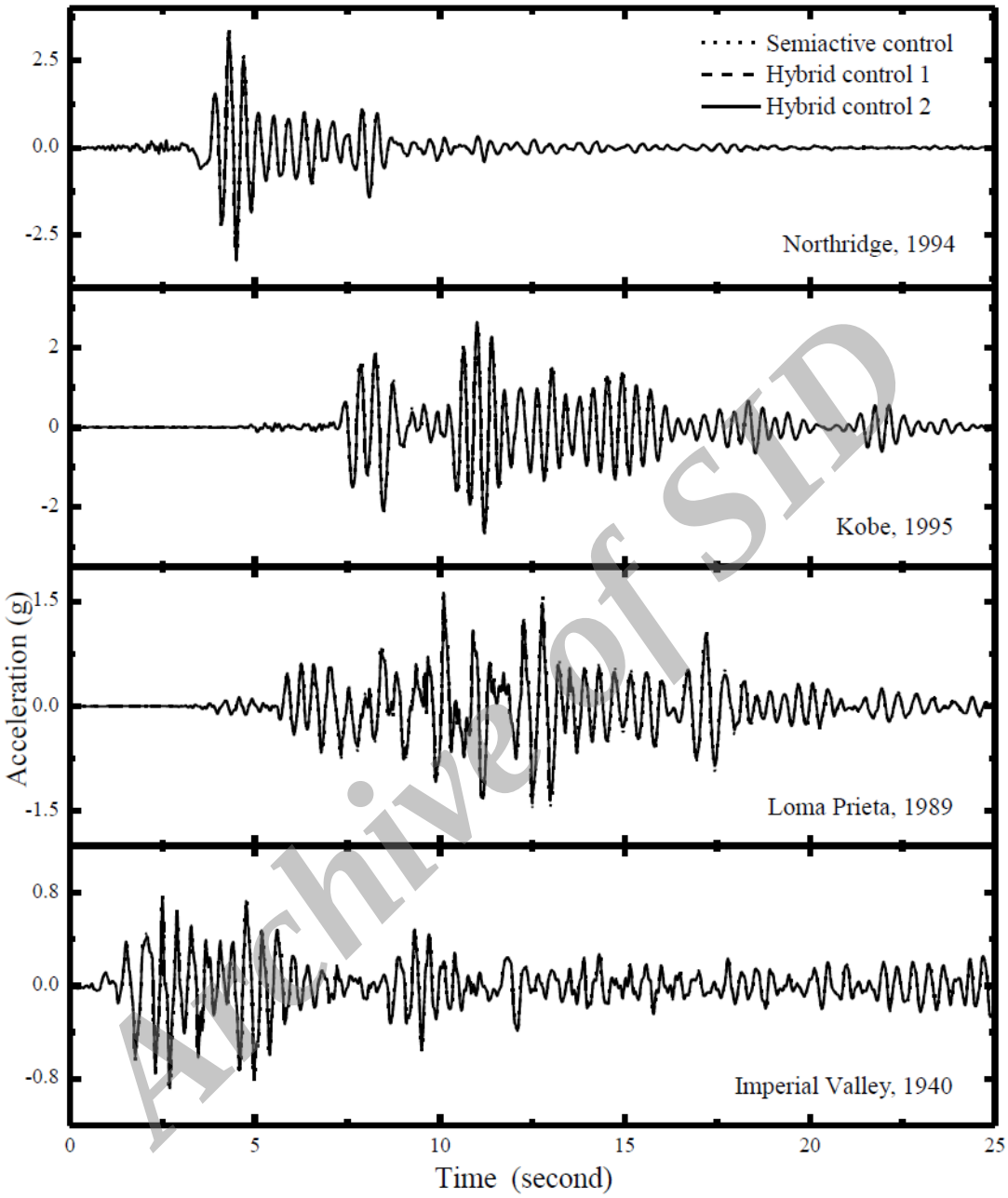

Figure 11. Time varying top floor acceleration of shorter building

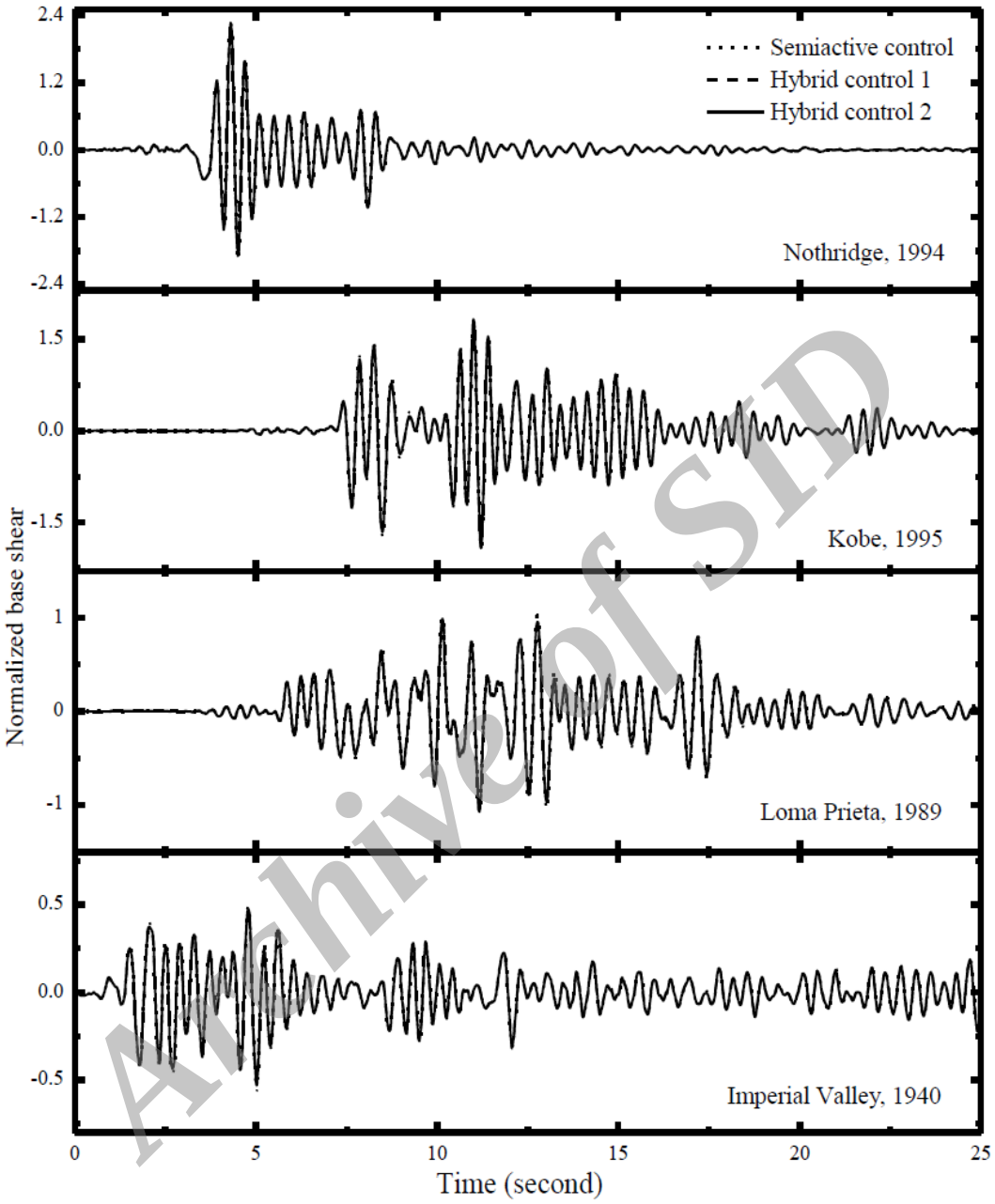

Figure 12. Time varying base shear of shorter building

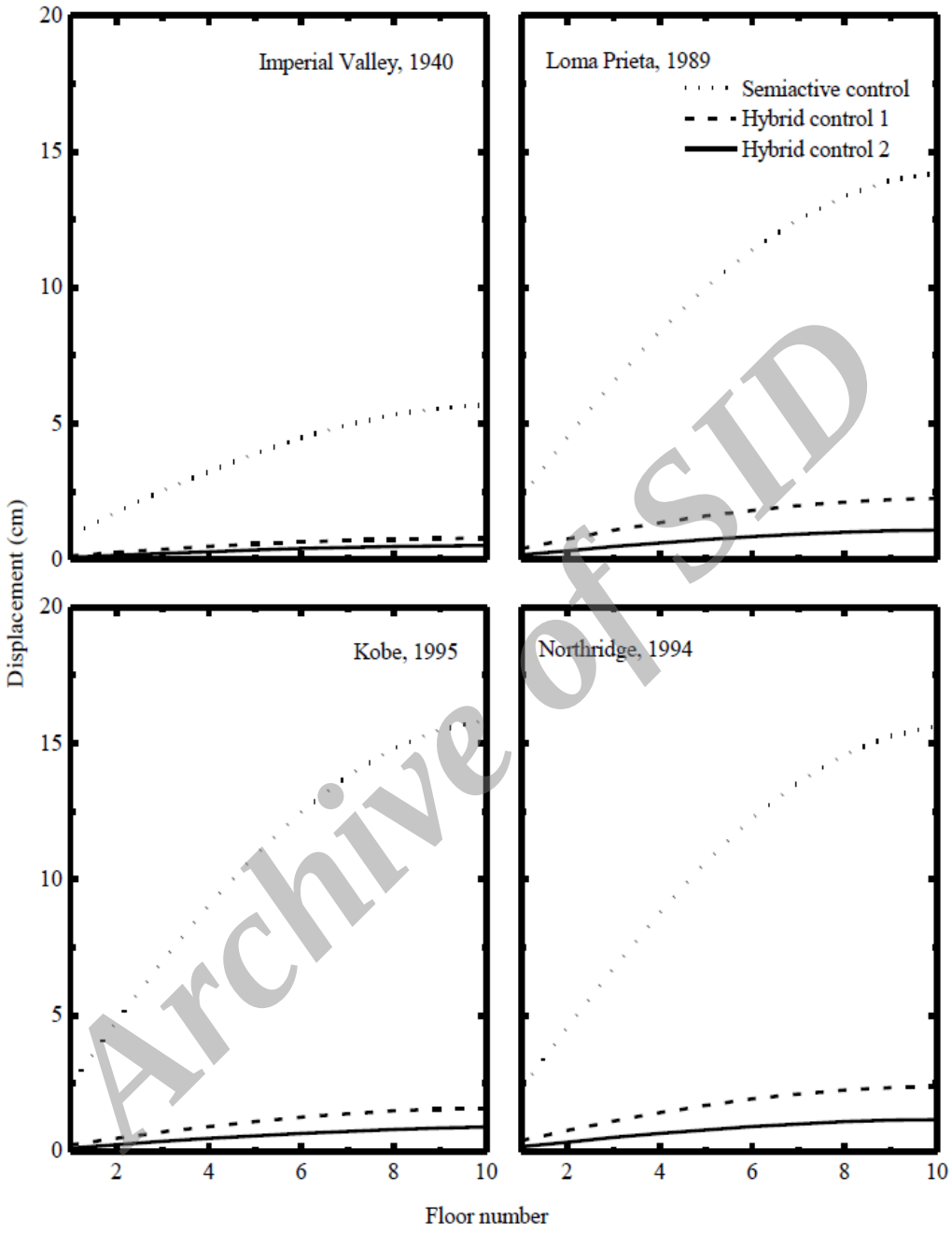

Figure 13. Peak displacement of each floor for taller building

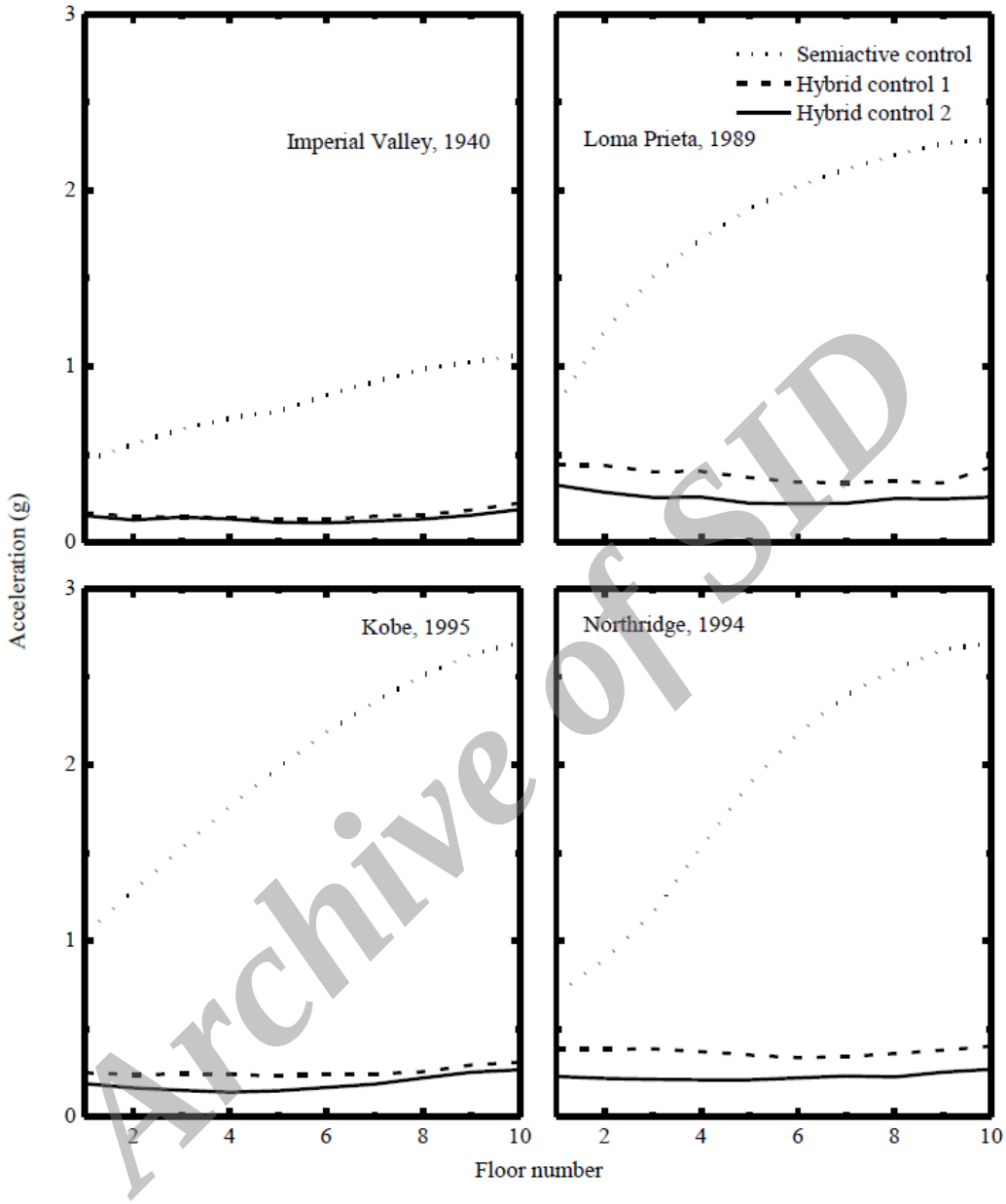

Figure 14. Peak acceleration of each floor for taller building

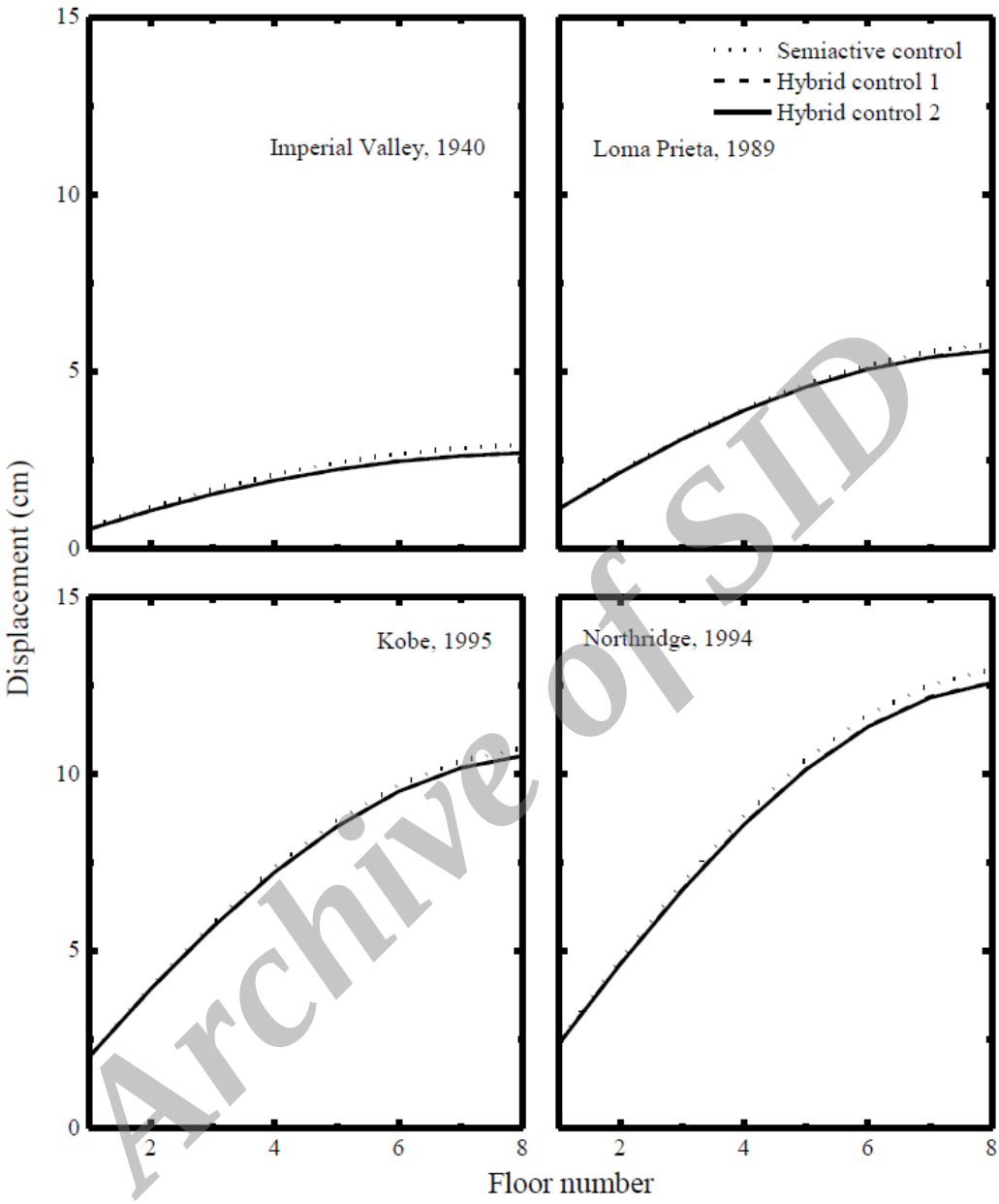

Figure 15. Peak displacement of each floor for shorter building

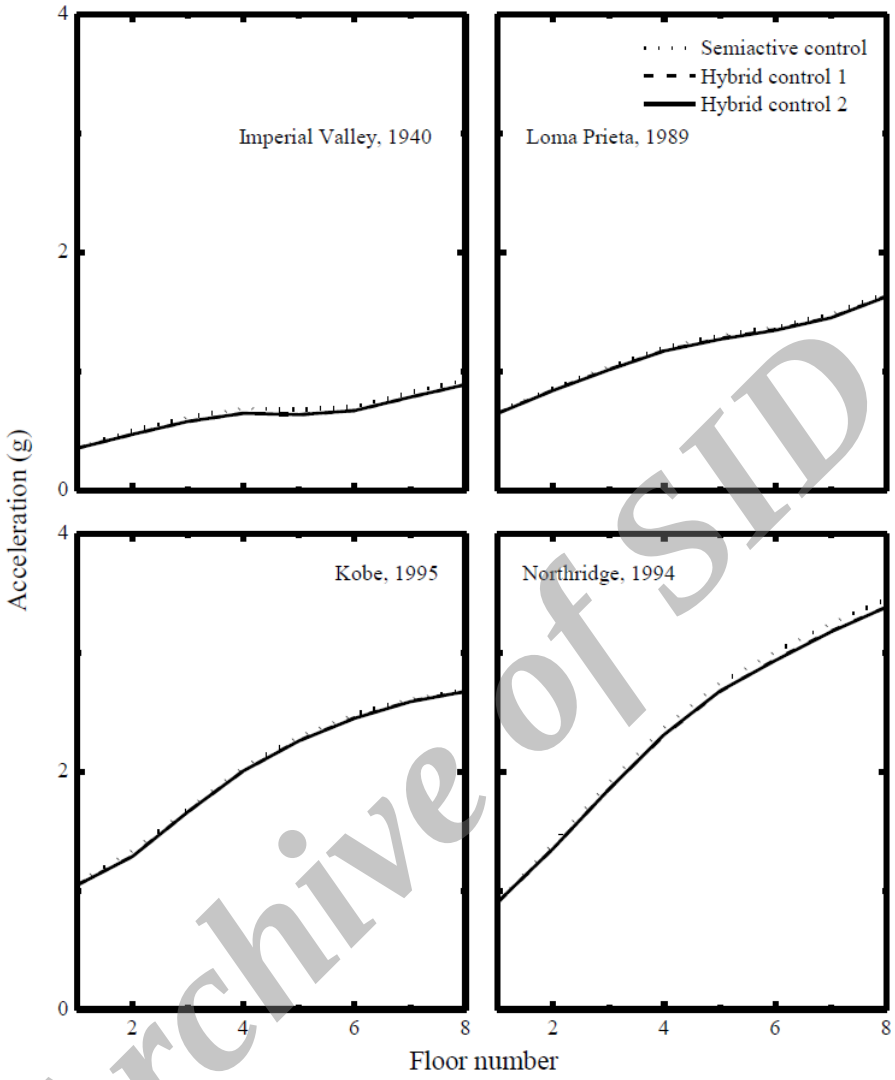

Figure 16. Peak acceleration of each floor for shorter building

For investigating the influence of damper command voltage on control performance, three values of voltage (3, 6, and 9V) has been chosen through a parametric study; results are shown in Table 2 and 3 for taller and shorter building respectively. It is noted that increase in damper voltage leads to better reduction in responses that is, displacement, acceleration and bearing displacement. Further, influence of damper location for three cases of damper locations is considered such as Case 1: all adjoining floors of shorter building are connected, Case 2: only 2^{nd}, 4^{th} 6^{th} and 8^{th} floors are connected whereas Case 3: only 2^{nd}, 5^{th} and 8^{th} floors are connected. The results of the same are mentioned in Table 4 and 5 in terms of peak responses for the taller and shorter buildings respectively. It has been noted that variation in response reduction across the three cases of damper location remains almost same; this shows that even if fewer dampers are provided the control strategy works well.

Table 2: Influence of damper command voltage on performance of hybrid controls for taller building

Earthquake	Peak response	Semi-active control			Hybrid control 1			Hybrid control 2		
		Damper command voltage			Damper command voltage			Damper command voltage		
		3V	6V	9V	3V	6V	9V	3V	6V	9V
EQ1	u_f	5.812	5.702	5.602	0.798	0.789	0.779	0.532	0.528	0.523
	a_f	1.074	1.0640	1.0553	0.2204	0.2219	0.2234	0.1889	0.1879	0.1869
	F_d	160.3	267.660	366.943	133.608	228.681	321.305	132.61	221.075	303.323
	u_b	-	-	-	5.255	5.179	5.702	5.280	5.203	5.129
EQ2	u_f	14.45	14.224	14.014	2.285	2.254	2.224	1.084	1.087	1.089
	a_f	2.2976	2.2848	2.2763	0.4305	0.4273	0.4236	0.2559	0.2574	0.2594
	F_d	347.57	584.515	805.867	231.451	393.236	548.193	231.976	392.744	545.477
	u_b	-	-	-	22.576	22.122	21.686	29.051	28.558	28.076
EQ3	u_f	16.140	15.862	15.725	1.620	1.589	1.559	0.896	0.902	0.908
	a_f	2.7495	2.6938	2.6516	0.3055	0.3124	0.3193	0.2629	0.2683	0.2795
	F_d	404.74	669.816	919.571	395.926	652.744	924.136	382.937	642.959	904.622
	u_b	-	-	-	12.032	11.768	11.501	10.197	10.162	10.123
EQ4	u_f	15.669	15.637	15.608	2.438	2.393	2.354	1.181	1.175	1.170
	a_f	2.6850	2.6944	2.7050	0.3940	0.4004	0.4067	0.2669	0.2720	0.2809
	F_d	479.81	823.115	1116.81	515.275	852.097	1246.299	475.852	805.497	1142.469
	u_b	-	-	-	22.728	22.231	21.761	19.071	18.783	18.496

Table 3: Influence of damper command voltage on performance of hybrid controls for shorter building

Earthquake	Peak response	Semi-active control			Hybrid control 1			Hybrid control 2		
		Damper command voltage			Damper command voltage			Damper command voltage		
		3V	6V	9V	3V	6V	9V	3V	6V	9V
EQ1	u_f	2.972	2.940	2.917	2.840	2.715	2.609	2.840	2.712	2.610
	a_f	0.9345	0.9264	0.9188	0.9123	0.8889	0.8659	0.9120	0.8891	0.8666
EQ2	u_f	5.768	5.795	5.949	5.722	5.603	5.491	5.719	5.593	5.479
	a_f	1.6859	1.6556	1.6279	1.673	1.6323	1.5940	1.6718	1.6279	1.5863
EQ3	u_f	11.022	10.726	10.465	10.912	10.525	10.160	10.907	10.518	10.153
	a_f	2.7741	2.6860	2.6135	2.7673	2.6733	2.5857	2.7648	2.6711	2.5812
EQ4	u_f	13.016	12.959	12.901	12.806	12.603	12.406	12.791	12.577	12.369
	a_f	3.4834	3.4496	3.4164	3.4434	3.3832	3.3243	3.4426	3.3804	3.3195

Table 4: Influence of damper location on performance of hybrid controls for taller building

Earthquake	Peak responses	Semi-active control			Hybrid control 1			Hybrid control 2		
		Case 1	Case 2	Case 3	Case 1	Case 2	Case 3	Case 1	Case 2	Case 3
EQ1	u_r (cm)	0.9071	0.9223	0.9274	0.1422	0.1438	0.1442	0.0868	0.0876	0.0881
	B_{sy}/W	0.7009	0.7103	0.7136	0.1205	0.1194	0.1191	0.0833	0.0812	0.0806
	u_b (cm)	--	--	--	5.1788	5.272	5.295	5.202	5.290	5.315
	F_d (kN)	267.6	278.616	282.352	228.681	231.714	232.667	221.075	230.429	233.576
EQ2	u_r (cm)	2.2971	2.3394	2.3539	0.3952	0.4037	0.4059	0.1771	0.1795	0.1802
	B_{sy}/W	1.7715	1.7984	1.8082	0.3029	0.3073	0.3083	0.1847	0.1826	0.1822
	u_b (cm)	---	--	--	22.122	22.707	22.856	28.557	29.221	29.424
	F_d (kN)	584.51	605.18	612.158	393.236	403.747	406.867	392.744	404.040	407.468
EQ3	u_r (cm)	2.4442	2.4606	2.4712	0.2535	0.2594	0.2609	0.1302	0.1315	0.1318
	B_{sy}/W	1.8980	1.9090	1.9121	0.2113	0.2075	0.2063	0.1490	0.1386	0.1362
	u_b (cm)	--	--	--	11.767	12.111	12.200	10.161	10.239	
	F_d (kN)	669.81	696.381	713.929	652.744	675.844	682.985	642.959	660.191	675.449
EQ4	u_r (cm)	2.2927	2.3020	2.3049	0.3960	0.4057	0.4078	0.1741	0.1758	0.1762
	B_{sy}/W	1.7886	1.782	1.7813	0.3107	0.3125	0.3131	0.1932	0.1874	0.1858
	u_b (cm)	--	--	--	22.231	22.829	22.977	18.767	19.160	19.272
	F_d (kN)	823.11	850.36	858.507	852.097	889.312	909.881	805.497	825.702	828.325

Table 5: Influence of damper location on performance of hybrid controls for shorter building

Earthquake	Peak responses	Semi-active control			Hybrid control 1			Hybrid control 2		
		Case 1	Case 2	Case 3	Case 1	Case 2	Case 3	Case 1	Case 2	Case 3
EQ1	u_r (cm)	0.6006	0.6044	0.6069	0.5551	0.5795	0.5882	0.5548	0.5794	0.5881
	B_{sy}/W	0.5663	0.5754	0.5790	0.5322	0.5558	0.5643	0.5319	0.5557	0.5642
EQ2	u_r (cm)	1.1386	1.1557	1.1618	1.1249	1.1479	1.1561	1.1237	1.1473	1.1556
	B_{sy}/W	1.0821	1.1010	1.1077	1.0741	1.0965	1.1043	1.0730	1.0960	1.1039
EQ3	u_r (cm)	2.0557	2.1117	2.1317	2.0113	2.0880	2.1138	2.0111	2.0873	2.1136
	B_{sy}/W	1.9443	2.0006	2.0205	1.9242	1.9912	2.0140	1.9220	1.9897	2.0130
EQ4	u_r (cm)	2.4434	2.4502	2.4527	2.3743	2.4102	2.4227	2.3693	2.4073	2.4195
	B_{sy}/W	2.3133	2.333	2.3401	2.2700	2.307	2.3205	2.2651	2.3047	2.3175

In addition to the above, parametric study also examined the influence of isolation parameters, namely, damping, friction coefficient and period on the seismic performance of hybrid controls in comparison to the Semi-active control. The influence of isolation damping on base shear of taller building and bearing displacement, under Hybrid control 2, is shown in Fig. 17; it is noted that increase in isolation damping leads to marginal increase in base shear, however, it causes decrease in bearing displacement. Fig. 18 portrays the effect of

friction coefficient, under Hybrid control 2 on base shear of taller building and bearing displacement. It is observed that increase in friction coefficient leads to decrease in bearing displacement and increase in base shear, however, sensitivity varies for each ground motion. The effect of isolation period on base shear of taller building and bearing displacement are shown in Figs. 19 and 20, respectively. It is observed from Fig. 19 that increases in isolation period upto 2s causes decrease in base shear, beyond which the effect becomes insignificant. Further, Fig. 20 indicates that increase in isolation period leads to increase in bearing displacement up to a certain value of isolation period, depending on ground motion characteristics. The hysteretic behaviour of top damper using Semi-active control and Hybrid controls for four earthquakes are presented through Figs. 21 and 22. Further, force-deformation behaviour of isolation systems for four same earthquakes is depicted through Figs. 23 and 24. It is noted that shape and size of hysteresis loop for the dampers and isolators renders the functioning of energy dissipation and reflection capacity found well.

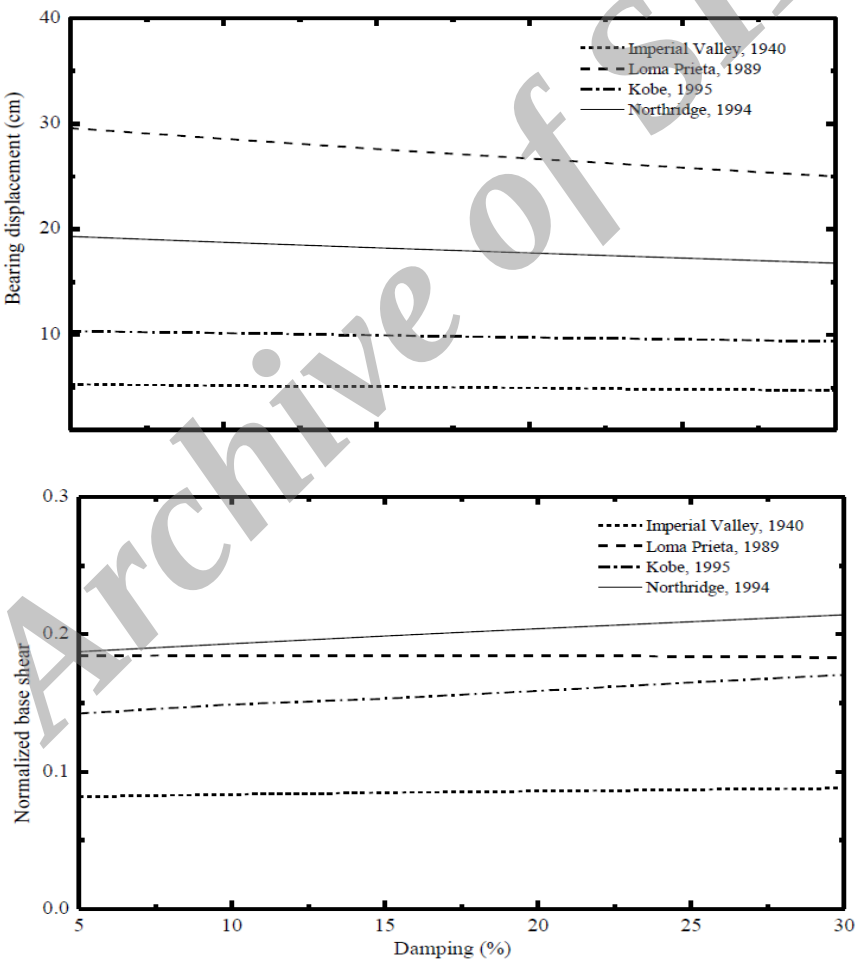

Figure 17. Effect of isolation damping on base shear and bearing displacement of taller building under hybrid control 2

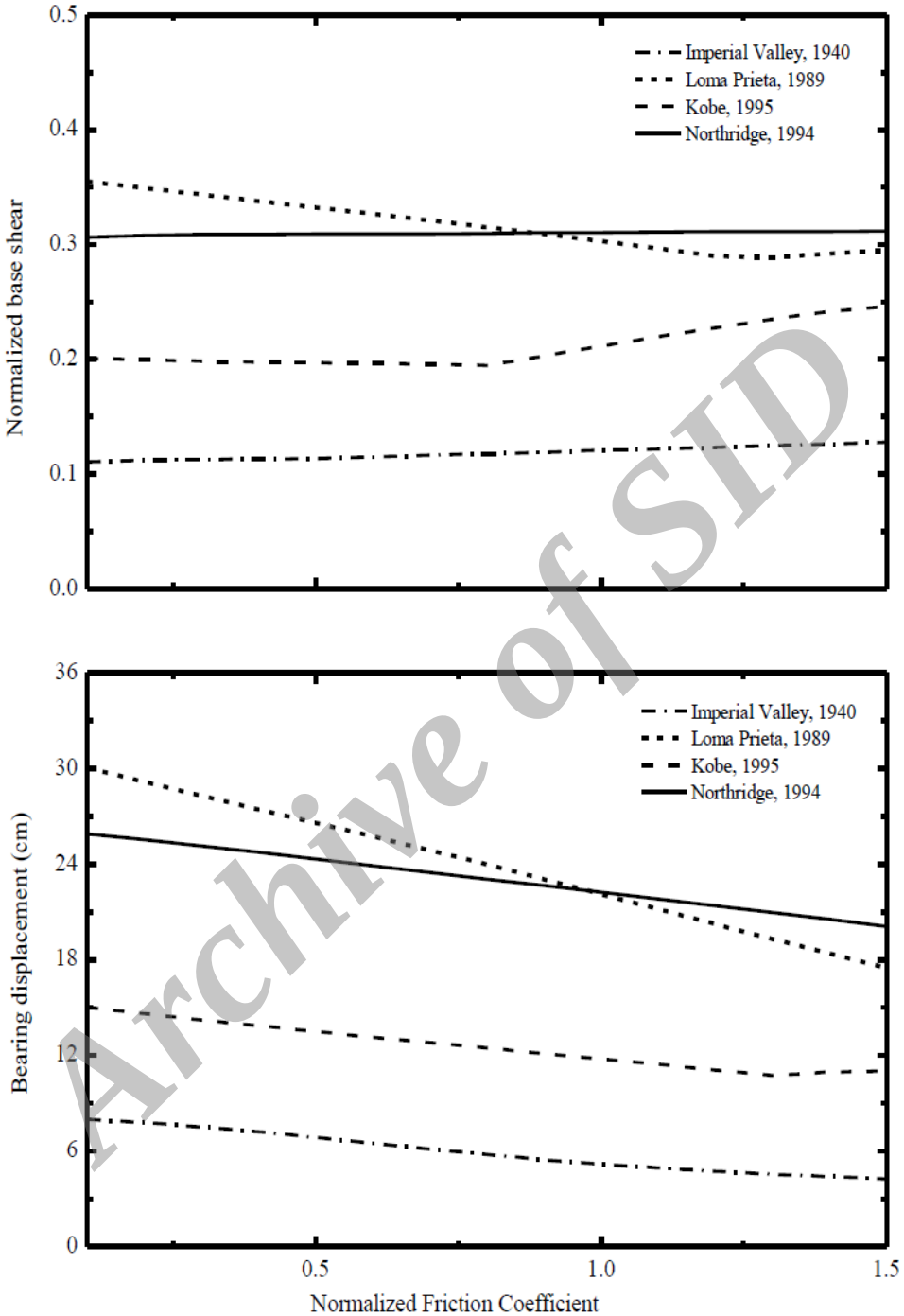

Figure 18. Effect of friction coefficient on base shear and bearing displacement for taller building under hybrid 2

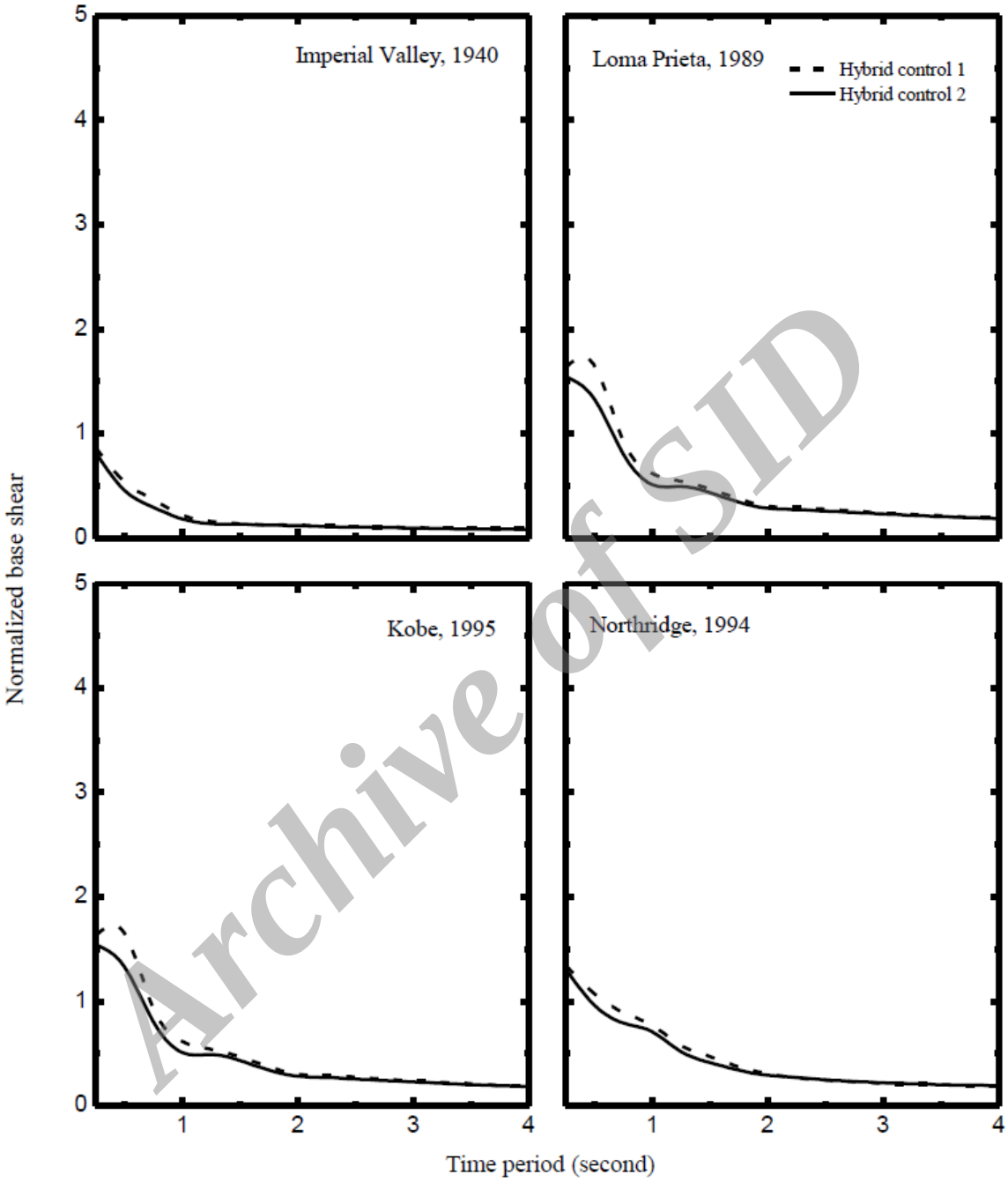

Figure 19. Effect of isolation period on base shear of taller building

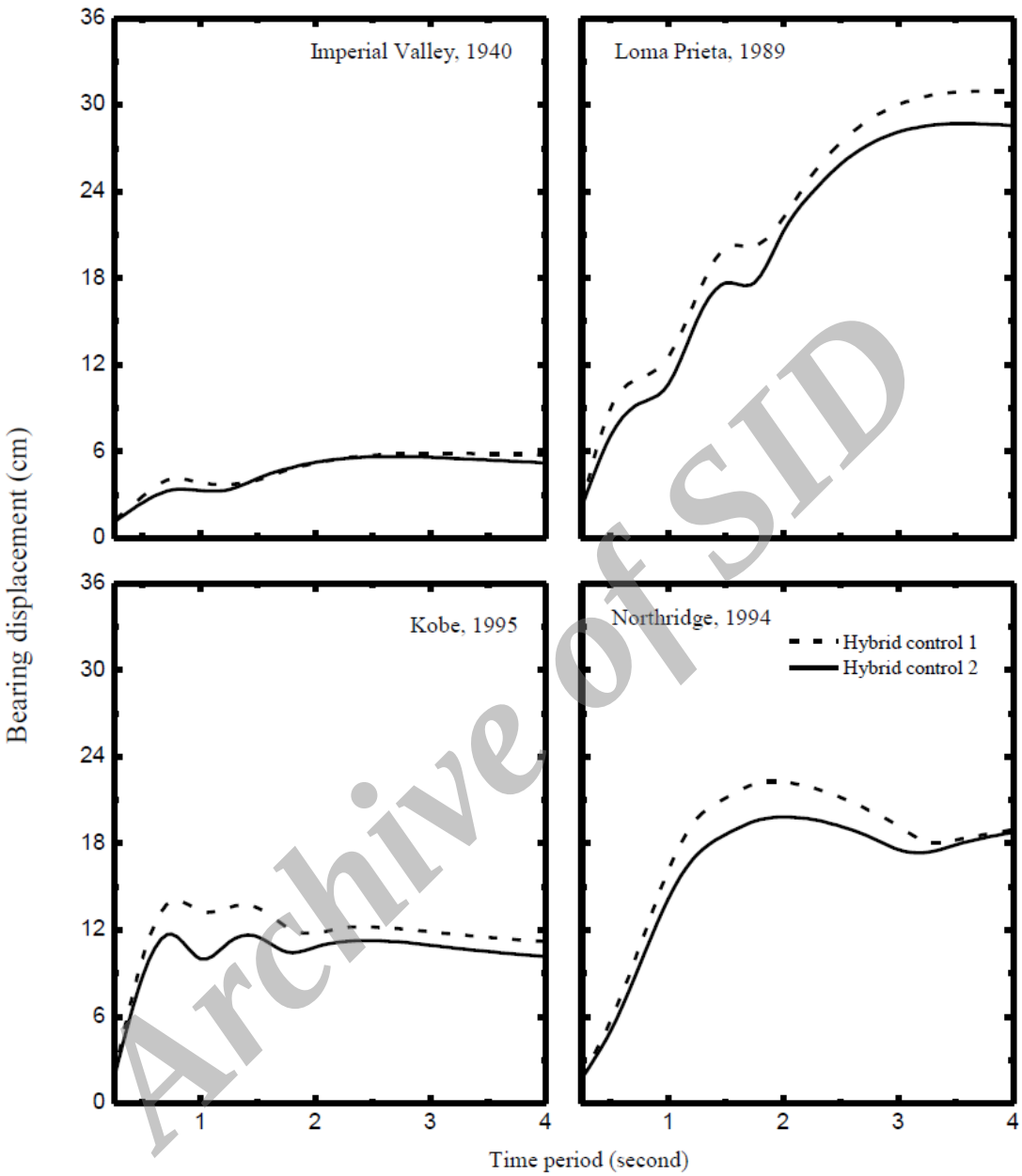

Figure 20. Effect of isolation period on peak bearing displacement

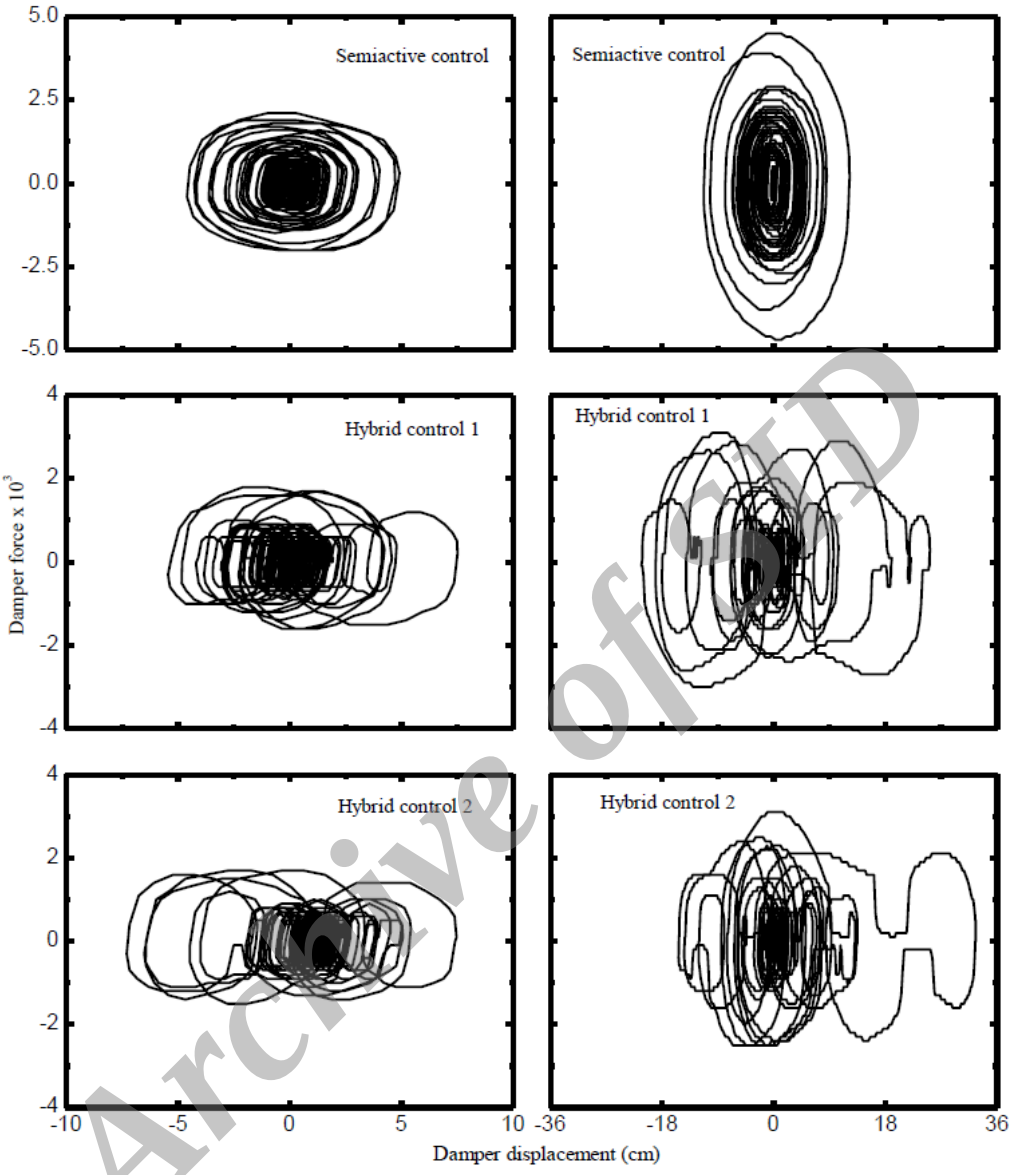

Figure 21. Force deformation behaviour of top MR damper

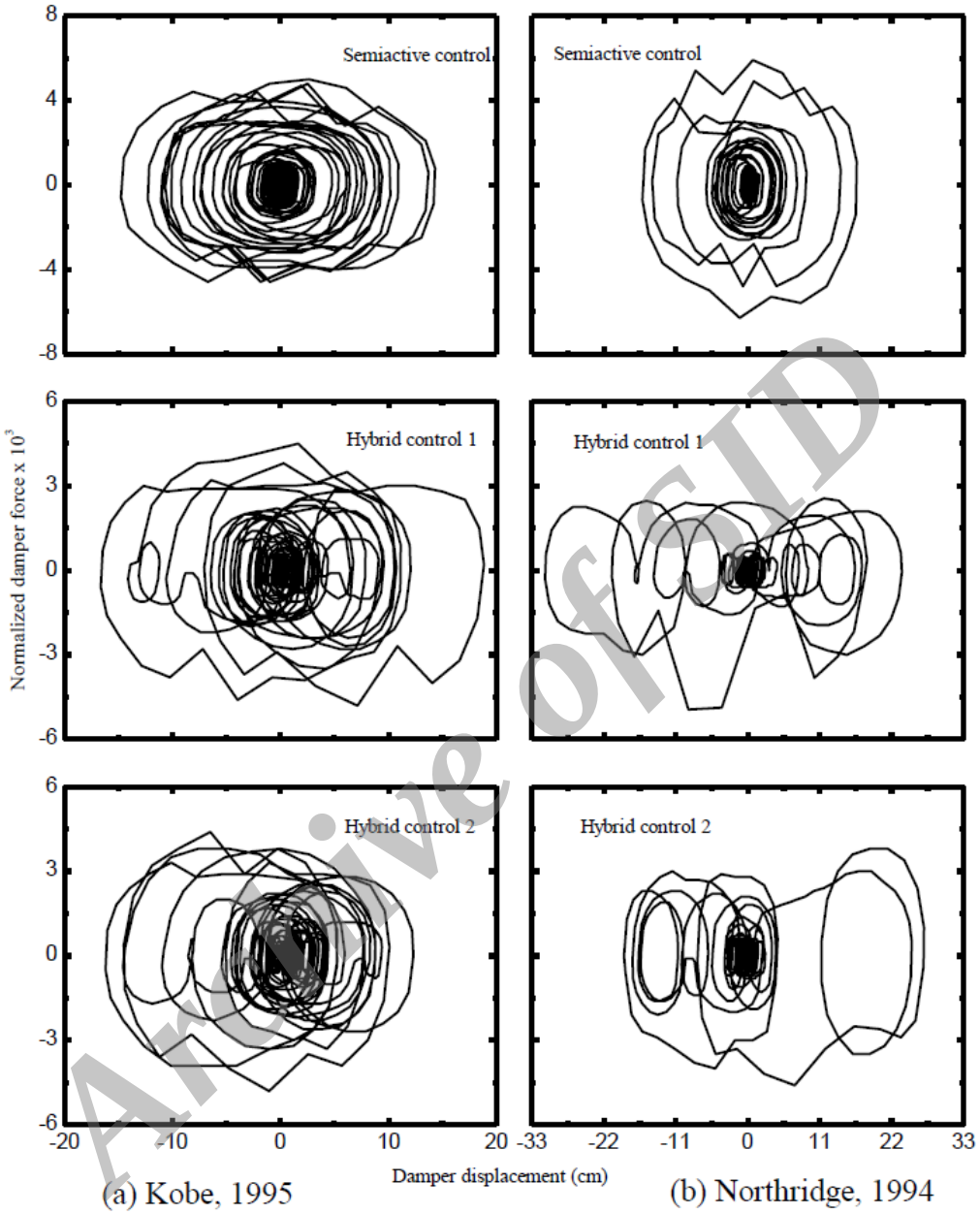

Figure 22. Force deformation behaviour of top damper

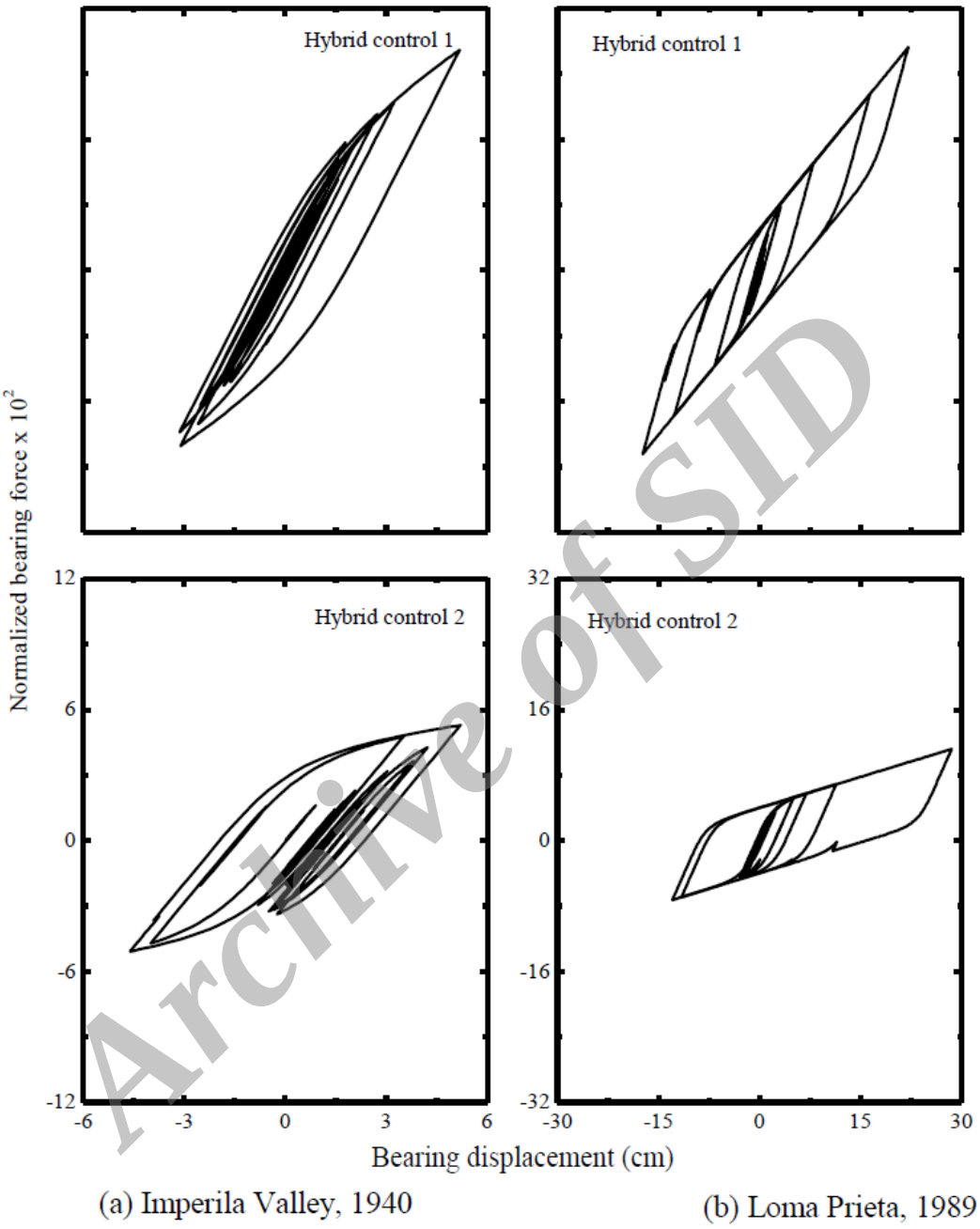

Figure 23. Force deformation behaviour of sliding base isolation systems

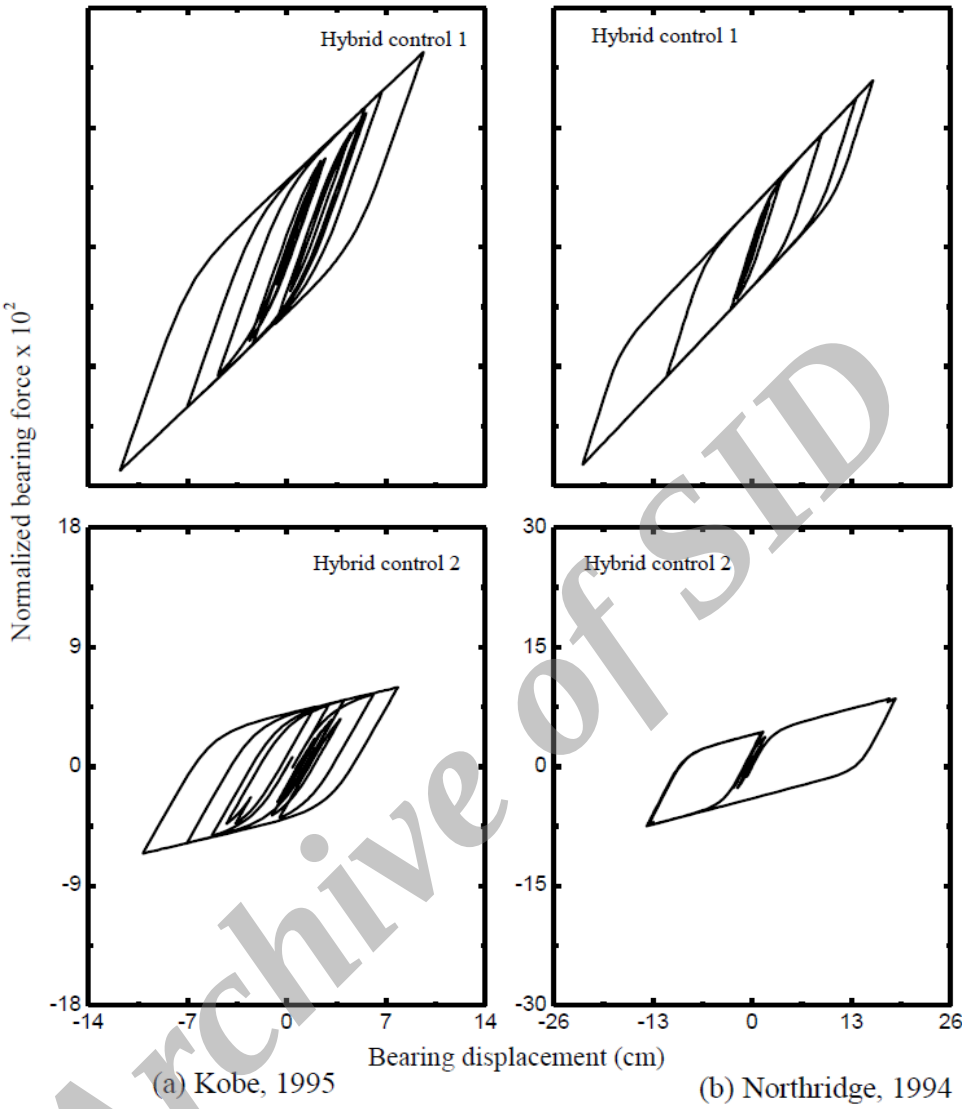

Figure 24. Force deformation behaviour of sliding base isolation systems

7. CONCLUSION

The coupling of two adjacent buildings by in-line MR dampers at each floors of shorter building of which base of taller building is isolated by sliding base isolators. The response of coupled building is evaluated using two hybrid control strategies in order to know its performance in comparison to Semi-active control. In addition, parametric study is also performed for the damper command voltage, damper location and isolation parameters, in order to understand the performance of hybrid controls. Based on trends of results from the numerical study, following conclusions are drawn.

1. Both the hybrid controls manifest significant reduction in responses of taller building whereas marginal reduction in shorter building as compared to Semi-active control.
2. Coupling two adjacent buildings at each floor of shorter building by dampers can results in response reduction even in the uncoupled floors.
3. Reduction in top floor and base shear responses under Hybrid control 1 and 2 are in close proximity.
4. The control over peak bearing displacement under Hybrid control 2 is better in comparison to Hybrid control 1 which implies that Hybrid control 2 is comparatively effective in preventing pounding.
5. Need to choose a suitable value of isolation period so as to keep the base shear and bearing displacement within acceptable range.
6. Increase in isolation damping leads to increase in base shear but slight decrease in bearing displacement.
7. Increase in friction coefficient leads to slight increase in base shear except for Loma Prieta, 1989 earthquake whereas decrease in bearing displacement.
8. Though fewer dampers are provided there is significant response reduction that takes place with the added advantage of saving the total cost of dampers.

Acknowledgements: The first author is grateful in expressing deep gratitude's to his Ph. D. supervisor Prof. M. K. Shrimali for his valuable guidance. Further, we hereby thanks to Prof. T. K. Datta and Prof. R. S. Jangid for their help and advices during this research work.

REFERENCES

1. Naserkhaki S, El-Rich M, Abdul Aziz FNA, Pourmohammad H. Separation gap, a critical factor in earthquake induced pounding between adjacent buildings, *Asian Journal of Civil Engineering (BHRC)*, No. 6, **14**(2013) 881-98.
2. Symans MD, Constantinou MC. Semi-active control systems for seismic protection of structures: state-of-the-art review, *Engineering Structures*, 21(1999) 469-87.
3. Jangid RS, Datta, TK. Seismic behaviour of base-isolated buildings: a state-of-the art review, *Proceedings of Institution of Civil Engineers, Structures and Buildings*, **110**(1995) pp. 186-203.
4. Bharti SD, Dumne SM, Shrimali MK. Earthquake response of asymmetric building with mr damper, *Earthquake Engineering and Engineering Vibration*, No. 13, **2**(2014) 305-16.
5. Bertero VV. Observations on structural pounding, in the Maxico Earthquakes, 1985, Factors Invilved and Lessons Learned, 1987, ASCE.
6. Westermo BD. The dynamics of interstructural connection to prevent pounding, *Earthquake Engineering & Structural Dynamics*, No. 18, **5**(1989) 687-99.
7. Zhang W, Xu Y. Dynamic characteristics and seismic response of adjacent buildings linked by discrete dampers, *Earthquake Engineering & Structural Dynamics*, No. 28, **10**(1999) 1163-85.
8. Zhu H, Xu Y. Optimum parameters of Maxwell model-defined dampers used to link adjacent structures, *Journal of Sound and Vibration*, No. 279, **1**(2005) 253-74.

9. Matsagar VA, Jangid RS. Viscoelastic damper connected to adjacent structures involving seismic isolation, *Journal of Civil Engineering and Management*, No. 11, **4**(2005) 309-22.
10. Bhaskararao AV, Jangid RS. Seismic analysis of structures connected with friction dampers, *Engineering Structures*, **28**(2006) 690-703.
11. Bharti SD, Dumne SM, Shrimali MK. Seismic response analysis of adjacent buildings connected with MR dampers, *Engineering Structures*, No. 32, **8**(2010) 2122-33.
12. Mate NU, Bakre S, Jaiswal O. Seismic pounding of adjacent linear elastic buildings with various contact mechanisms for impact simulation, *Asian Journal of Civil Engineering (BHRC)*, No. 16, **3**(2015) 383-415.
13. Abdeddaim M, Ounis A, Djedoui N, Shrimali MK. Reduction of Pounding between Buildings using Fuzzy Controller, *Asian Journal of Civil Engineering (BHRC)*, No. 16, **3**(2015) 383-415.
14. Shrimali MK, Bharti SD, Dumne SM. Seismic response analysis of coupled building involving MR dampers and elastomeric base isolation, *Ain Shams Engineering Journal*, **6**(2015) 457-70.
15. Dumne SM, Bharti SD, Shrimali MK. Seismic performance of coupled building connected by Semi-active MR Dampers involving resilient-friction base isolator, *Proceeding of Third International Conference on Recent Trends in Engineering & Technology (ICRTET 2014)*, Elsevier, ISBN: 978-93-5107-222-5, 28-30 March 2014.
16. Spencer Jr BF, Dyke SJ, Sain MK, Carlson JD. Phenomenological model for Magnetorheological dampers, *Journal of Engineering Mechanics, ASCE*, No. 123, **3**(1997) 230-38.
17. Dyke SJ, Spencer Jr BF, Sain MK, Carlson JD. Modeling and control of Magnetorheological dampers for seismic response reduction, *Smart Materials and Structures*, **5**(1996) 565-75.
18. Constantinou MC, Tadjbakhsh IG. The optimum characteristics of isolated structures, *Journal of Structural Engineering, ASCE*, No. 111, **12**(1985) 2733-50.
19. Wen YK. Method for random vibration of hysteretic systems, *Journal of Engineering Mechanics Division, ASCE*, No. 102, **2**(1976) 249-63.
20. Mostaghel N, Khodaverdian M. Dynamics of resilient-friction base isolator (R-FBI), *Earthquake Engineering and Structural Dynamics*, No. 15, **3**(1987) 379-390.